Molecular Therapy
Original Article

MANF Promotes Differentiation and Migration of Neural Progenitor Cells with Potential Neural Regenerative Effects in Stroke

Kuan-Yin Tseng,[1,2] Jenni E. Anttila,[1] Konstantin Khodosevich,[3] Raimo K. Tuominen,[4] Maria Lindahl,[1] Andrii Domanskyi,[1] and Mikko Airavaara[1]

[1]Institute of Biotechnology, HiLIFE Unit, University of Helsinki, Helsinki, Finland; [2]Department of Neurological Surgery, Tri-Service General Hospital and National Defense Medical Center, Taipei, Taiwan; [3]Biotech Research and Innovation Centre, University of Copenhagen, Copenhagen, Denmark; [4]Division of Pharmacology and Pharmacotherapy, Faculty of Pharmacy, University of Helsinki, Helsinki, Finland

Cerebral ischemia activates endogenous reparative processes, such as increased proliferation of neural stem cells (NSCs) in the subventricular zone (SVZ) and migration of neural progenitor cells (NPCs) toward the ischemic area. However, this reparative process is limited because most of the NPCs die shortly after injury or are unable to arrive at the infarct boundary. In this study, we demonstrate for the first time that endogenous mesencephalic astrocyte-derived neurotrophic factor (MANF) protects NSCs against oxygen-glucose-deprivation-induced injury and has a crucial role in regulating NPC migration. In NSC cultures, MANF protein administration did not affect growth of cells but triggered neuronal and glial differentiation, followed by activation of STAT3. In SVZ explants, MANF overexpression facilitated cell migration and activated the STAT3 and ERK1/2 pathway. Using a rat model of cortical stroke, intracerebroventricular injections of MANF did not affect cell proliferation in the SVZ, but promoted migration of double-cortin (DCX)$^+$ cells toward the corpus callosum and infarct boundary on day 14 post-stroke. Long-term infusion of MANF into the peri-infarct zone increased the recruitment of DCX$^+$ cells in the infarct area. In conclusion, our data demonstrate a neuroregenerative activity of MANF that facilitates differentiation and migration of NPCs, thereby increasing recruitment of neuroblasts in stroke cortex.

INTRODUCTION

Neurogenesis persists in the adult rodent brain within the subventricular zone (SVZ) and the subgranular layer of the hippocampus.[1–3] Neural stem cells (NSCs) of the SVZ give rise to neural progenitor cells (NPCs) that migrate through the rostral migratory stream to the olfactory bulb, where they differentiate into granule and periglomerular neurons throughout the adult life of rodents.[4,5] Ischemic injury drastically increases neurogenesis in the rodent SVZ,[6] and the surviving neuroblasts migrate out of the SVZ into the striatum and mature into functional neurons.[7] Moreover, transient angiogenesis after stroke allows neuroblasts to migrate along newly formed blood vessels, aiding in their migration out of the SVZ.[8] In the model of cortical stroke, the majority of NPCs either fail to reach the lesioned cortex or differentiate into glial cells due to a non-permissive environment for neuronal differentiation.[9,10] Therefore, attempts to utilize the therapeutic potential of these cells to replace lost neurons in the infarct cortex have had limited success.[11,12]

Small secreted proteins, such as growth factors, regulate survival, differentiation, and maturation of neurons during development.[13] In the adult brain, they support the survival of neurons and regeneration of axons after injury,[14] making them good candidates to be used for enhancing recovery after stroke. For example, glial cell line-derived neurotrophic factor (GDNF) and GDNF family receptor alpha 1 (GFRα1) promote differentiation and tangential migration of cortical GABAergic neurons during brain development.[15] Additionally, GDNF has a chemoattractant effect in the migration of neuronal precursor cells along the rostral migratory stream (RMS),[16] and studies on GFRα1 knockouts demonstrate its role in the development and function of the olfactory system.[17]

In the stroke model, GDNF was found to promote the proliferation of NPCs in the SVZ and their recruitment into the damaged striatum.[18] Similarly, administration of brain-derived neurotrophic factor (BDNF) stimulates post-stroke neurogenesis.[19] Additionally, our previous data demonstrate that adeno-associated virus (AAV)-BDNF transduction enhances the migration of SVZ cells toward the lesioned hemisphere in stroke rats.[20]

Unlike GDNF or BDNF, mesencephalic astrocyte-derived neurotrophic factor (MANF), together with its homolog cerebral dopamine neurotrophic factor (CDNF), are non-classical neurotrophic factors that reside in the endoplasmic reticulum (ER) and are secreted from cells in response to ER stress.[21–25] MANF has been shown to be upregulated by the unfolded protein response (UPR) and

Received 2 July 2017; accepted 18 September 2017;
https://doi.org/10.1016/j.ymthe.2017.09.019.

Correspondence: Mikko Airavaara, PhD, Institute of Biotechnology, University of Helsinki, P.O. Box 56 (Viikinkaari 5D), 00014 Helsinki, Finland.
E-mail: mikko.airavaara@helsinki.fi

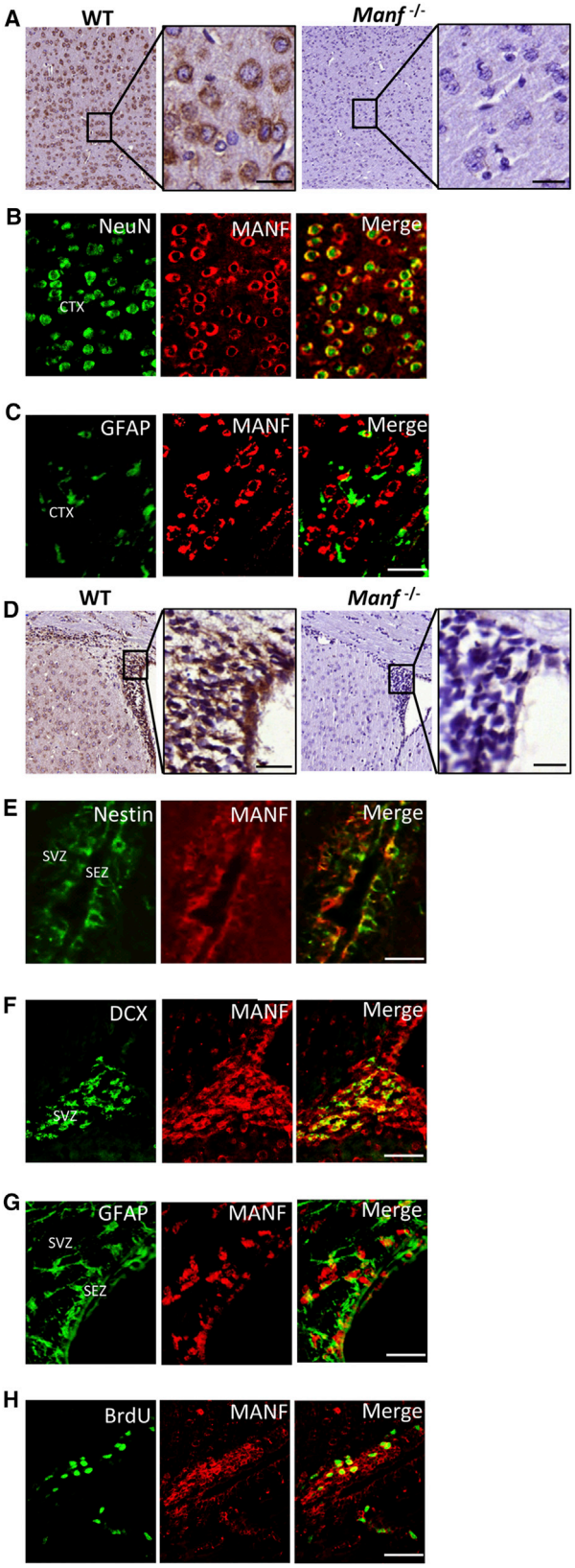

Figure 1. MANF Expression in the P35 Mouse Brain

(A) Coronal cortical sections from P35 brains stained with MANF antibody from WT and *Manf*$^{-/-}$ mice. The insets show photomicrographs of the cortex at higher magnification and immunostained with MANF antibody. (B and C) Double immunofluorescent labeling was performed to determine the localization of MANF (red). Neurons and astrocytes were identified by NeuN (B) and GFAP (C) (green), respectively. (D) Photomicrographs of coronal sections of the SVZ and striatum stained with MANF antibody from WT and *Manf*$^{-/-}$ mice. The insets show the SVZ at higher magnification immunoreactive for MANF antibody. (E) SEZ and SVZ double-labeled for Nestin (green) and MANF (red) antibodies. (F) Section of SVZ from adult mouse double-labeled with DCX (green) and MANF (red) antibodies. (G) Coronal sections of the SEZ and SVZ stained with GFAP (green) and MANF (red) antibodies; (H) for BrdU (green) and MANF (red) antibodies. Scale bars, 20 μm (A and D inset) and 50 μm (C and E–H). CTX, cerebral cortex; SEZ, subependymal zone.

stroke,[21,22,26] and lack of MANF leads to chronic UPR in the pancreatic islets in vivo.[27] We previously demonstrated that MANF has a neuroprotective effect in the distal middle cerebral artery occlusion (dMCAo) model of cerebral ischemic injury.[28,29] Recently, MANF has been shown to promote tissue repair and improve the success of photoreceptor replacement therapies in the damaged retina.[30]

In this study, we first aimed to characterize the effects of MANF on NSCs in the homeostatic condition and with a stress insult. We determined the role of MANF in NPC migration and its possible molecular mechanisms by administration of exogenous MANF or by modifying *Manf* expression levels in in vitro SVZ explants. Furthermore, we used an in vivo cortical stroke model to test the effect of MANF in neuroblast migration from the SVZ.

RESULTS

MANF Is Expressed in Both Mitotic NSCs and NPCs and Post-mitotic Neurons in the Adult Brain

The specificity of MANF antibodies was validated by comparing wild-type (WT) and *Manf*$^{-/-}$ cortical sections. We found MANF expression in the cerebral cortex of WT but not *Manf*$^{-/-}$ mice (Figure 1A). MANF was co-localized with NeuN, but not with glial-associated intermediate filament (GFAP), in the cortex of a mature mouse brain (Figures 1B and 1C), suggesting that MANF protein was mainly expressed in mature neurons. Notably, MANF was also strongly expressed in the adult SVZ of WT mice (Figure 1D) and co-localized with Nestin, doublecortin (DCX), and GFAP (Figures 1E–1G). Importantly, BrdU^{+} cells in the SVZ also expressed MANF (Figure 1H). These results show that MANF is not only expressed in mature cortical neurons, but also in SVZ cells, including quiescent NSCs (type B cells, GFAP^{+}), transient amplifying progenitors (type C cells, Nestin^{+}), and neuroblasts (type A cells, DCX^{+}) of the adult brain.

Administration of MANF Does Not Affect Growth or Self-Renewal of NSCs but Triggers Neuronal and Glial Differentiation

A strong immunofluorescent signal for MANF was found in the cultured WT NSCs, and no signal was observed in *Manf*$^{-/-}$ cells (Figure 2A). First, we analyzed the diameter of neurospheres and found no difference in the size of neurospheres between WT and *Manf*$^{-/-}$

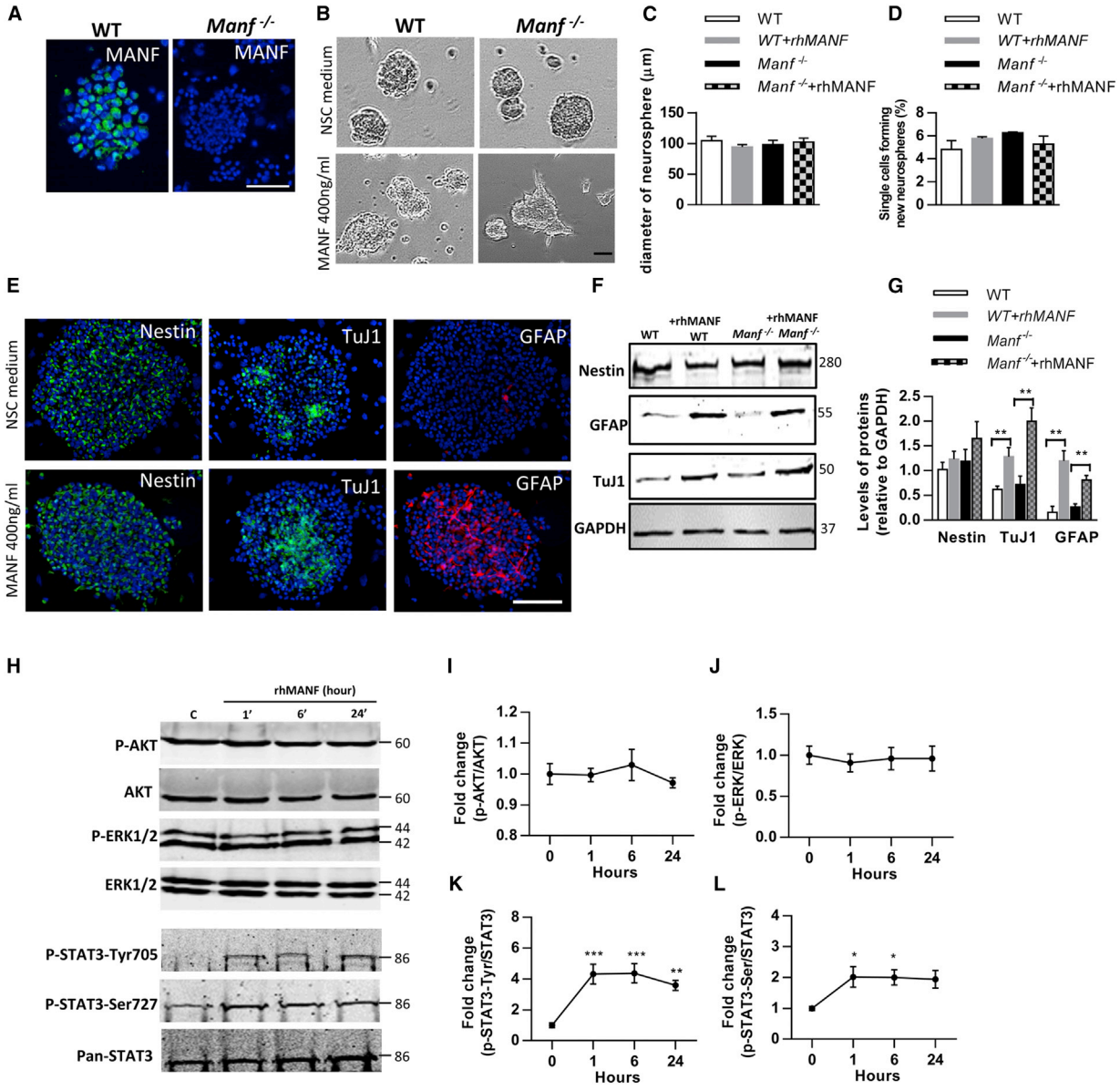

Figure 2. MANF Stimulates STAT3 Signaling Pathways in NSC/NPC Cultures

(A) Immunofluorescent staining against MANF (green) shows high signal in WT and no signal in *Manf*$^{-/-}$ neurospheres. (B) Representative images of the neurospheres in 24-well plates on DIV5. Treatment with rhMANF (400 ng/mL) induced morphological changes in WT and *Manf*$^{-/-}$ neurospheres, including asymmetrical conformation and induction of neurite-like processes. (C) Administration of rhMANF (400 ng/mL) did not increase the diameter of neurospheres derived from WT and *Manf*$^{-/-}$ mice. (D) Administration of exogenous MANF to WT or MANF-deficient cells does not affect the proportion of self-renewing NSCs (n = 8). The ability of single cells to form new neurospheres was evaluated after 7 days of culture in EGF/FGF-containing stem cell medium. (E) Representative photomicrographs of NSC/NPCs in neurospheres labeled for Nestin (green), TuJ1 (green), or GFAP (red), and nuclei were counterstained with DAPI (blue). (F) Lysates from WT and MANF$^{-/-}$ NPCs, treated with vehicle or rhMANF for 4 days, subjected to immunoblot analysis to determine levels of tubulin (TuJ1) and GFAP. (G) Protein levels were quantified as relative levels compared to GAPDH, n = 3, Student's t test, **p < 0.01. (H) Neurospheres, grown in the NSC medium, were incubated with rhMANF (400 ng/mL) for 0, 1, 6, and 24 hr. Thereafter, lysates were prepared and western blot was performed using the indicated antibodies. (I and J) The presence of rhMANF did not increase the phosphorylation of AKT or ERK1/2 in neurospheres. P-AKT (I) and p-ERK (J) were normalized to AKT and ERK, respectively. The levels are shown as fold change to control cells. (K) rhMANF induced sustained p-STAT3-Tyr705 increase that lasted until 24 hr. P-STAT3-Tyr were normalized to Pan-STAT3 and presented as fold change to control (n = 5, one-way ANOVA, p = 0.004; ***p < 0.001; **p < 0.01). (L) rhMANF increased phosphorylation of STAT3-Ser727 that lasted until 6 hr. P-STAT3-Ser was normalized to Pan-STAT3 and presented as fold change to control cells (n = 5, one-way ANOVA, p = 0.03; *p < 0.05). Scale bars, 50 μm (A) and 100 μm (B and E). Data are presented as mean ± SEM.

groups (Figures 2B and 2C), indicating that loss of MANF did not affect growth of neurospheres. Next, we studied the effect of endogenous MANF on self-renewal of NSCs and found there was a similar self-renewal rate of NSCs between the genotypes. Single cell suspension of WT or Manf$^{-/-}$ NSCs were treated either with recombinant human MANF (rhMANF) (400 ng/mL) or vehicle (PBS), and we did not observe any effects of exogenous rhMANF on the percentage of NSCs forming new neurospheres (Figure 2D). However, many rhMANF-treated WT and *Manf*$^{-/-}$ NSCs showed localized budding and cellular process extensions, implying that the cells had undergone morphological changes (Figure 2B). Immunofluorescence revealed stronger expression of TuJ1, a marker for neuron-specific tubulin, and GFAP, an intermediate filament marker for glial cells, in rhMANF-treated neurospheres (Figure 2E). Moreover, western blot analysis revealed increased levels of TuJ1 and GFAP in rhMANF-treated neurospheres compared to non-treated, but Nestin levels were similar between the groups (Figures 2F and 2G). Previously, MANF and CDNF have been reported to act like classical neurotrophic factors (NTFs) by extracellularly promoting cell survival via activation of the PI3K-AKT pathway.[31,32] To test whether the trophic effects of MANF on NSCs are mediated through AKT or other pathways, neurospheres were treated with 400 ng/mL rhMANF for 0, 1, 6, and 24 hr (Figure 2H). However, the time-course analysis revealed that rhMANF did not trigger AKT or ERK1/2 activation (Figures 2I and 2J). Interestingly, addition of rhMANF to NSCs revealed a 4-fold increase in phosphorylation of STAT3 tyrosine705 (Figure 2K). The increase was observed at 1 hr and the levels remained high until 24 hr after MANF administration. Also, rhMANF stimulated the phosphorylation of STAT3 on Ser727 and there was a significant increase at 1 and 6 hr after MANF addition, but there was no statistically significant increase at the 24-hr time point (Figure 2L). Together, these results demonstrate that endogenous and exogenous MANF do not affect the growth or self-renewal of NSCs, but exogenous MANF triggered neuronal and glial differentiation, which was accompanied by increased STAT3 phosphorylation.

Loss of MANF Increases NSC Vulnerability to OGD- and Reoxygenation-Induced Stress

Previously, MANF has been shown to rescue neurons from apoptosis.[28,33,34] Therefore, we investigated whether MANF had a protective effect on NSC under 40 min of oxygen-glucose deprivation (OGD), followed by 24 hr re-oxygenation (Figure 3A). We quantified the proportion of activated caspase-3$^+$ cells and found significantly increased numbers of activated caspase-3$^+$ cells in *Manf*$^{-/-}$ NSCs compared to WT (Figures 3B and 3C). Moreover, the apoptotic rate in *Manf*$^{-/-}$ NSCs exposed to OGD and reoxygenation was decreased with rhMANF treatment (Figures 3B and 3C). Next, we used propidium iodide (PI) staining to re-assess the viability of WT and *Manf*$^{-/-}$ NSCs. In normoxic conditions, the percentage of apoptotic cells was similar between WT and *Manf*$^{-/-}$cells (Figure 2K, 24.9% ± 2.9 [n = 6] versus 25.2% ± 1.3 [n = 6], respectively). However, after 40 min OGD and 24 hr reoxygenation, the proportion of dying *Manf*$^{-/-}$ cells was significantly higher compared to dying WT cells (Figure 3D). Moreover, pre-treatment of rhMANF significantly decreased the percentage of PI$^+$ *Manf*$^{-/-}$ cells (Figure 3D), indicating that administration of rhMANF could partially rescue *Manf*$^{-/-}$ cells from dying. Taken together, the above data suggest that deletion of MANF increases vulnerability of NSCs to OGD-induced stress and administration of rhMANF could, at least partially, compensate for the lack of MANF in *Manf*$^{-/-}$ NSCs.

MANF Regulates Cell Migration in SVZ Explants

Next, we examined whether endogenous MANF is involved in the neuronal migration, a critical step in brain development. We isolated the SVZ fragments from WT and *Manf*$^{-/-}$ embryos (E19) and cultivated these in Matrigel to investigate the migration of cells from SVZ explants. At days in vitro 2 (DIV2), few cells had migrated from the explant (Figures 4A and 4B). At DIV7, many cells were found in the periphery of the WT explant. However, cells lacking MANF showed a shorter distance of migration (Figures 4A and 4B) compared to WT cells. These data suggest that endogenous MANF is essential for migration of cells from SVZ explants in vitro.

Because endogenous MANF is essential for embryonic SVZ cell migration in vitro, we investigated whether administration of rhMANF further promotes cell migration from the postnatal SVZ explants. SVZ explants collected from mouse brains were treated daily with rhMANF (0, 200, 400, and 800 ng/mL) or BDNF (25 ng/mL, positive control) on days 1–4. At DIV1, there was minimal migration of cells (Figure 4C). At DIV4, treatment with 400 ng/mL MANF or BDNF increased the cell migration distance (Figures 4C and 4D). At DIV7, administration of MANF (200 and 400 ng/mL) increased the distance of cell migration from SVZ explants when compared to the vehicle group. However, rhMANF at a dose of 800 ng/mL did not increase cell migration from SVZ explants (Figure 4D), implying that exogenous MANF regulates cell migration in a dose-dependent manner.

Overexpression of MANF Enhanced DCX$^+$ Cell Migration from SVZ Explants

Next, we investigated whether the lentivirus (LV)-mediated overexpression of hMANF in DCX$^+$ cells induced their migration from SVZ explants. As a control, we overexpressed a membrane-targeted myristoylated serine-threonine protein kinase Akt1 that causes constitutive activation of the Akt signaling pathway[35] because the Akt pathway has been shown to mediate migration of developing neurons. In order to test the function of LV preparations, developing cortical neurons were transduced with LV-hDCX-GFP, LV-hDCX-myrAKT-GFP, and LV-hDCX-hMANF-IRES-GFP. 5 days after transduction we observed GFP fluorescence (green) in DCX$^+$ cells (red), which was indicative of successful transduction (Figures 5A–5C). Using a sensitive ELISA, we found that hMANF concentrations were significantly increased in cortical neuronal lysates (Figure 5D) and in media (Figure 5E) after LV-hDCX-hMANF-IRES-GFP treatment when compared to neurons transduced by LV-hDCX-GFP or LV-hDCX-myrAKT-GFP.

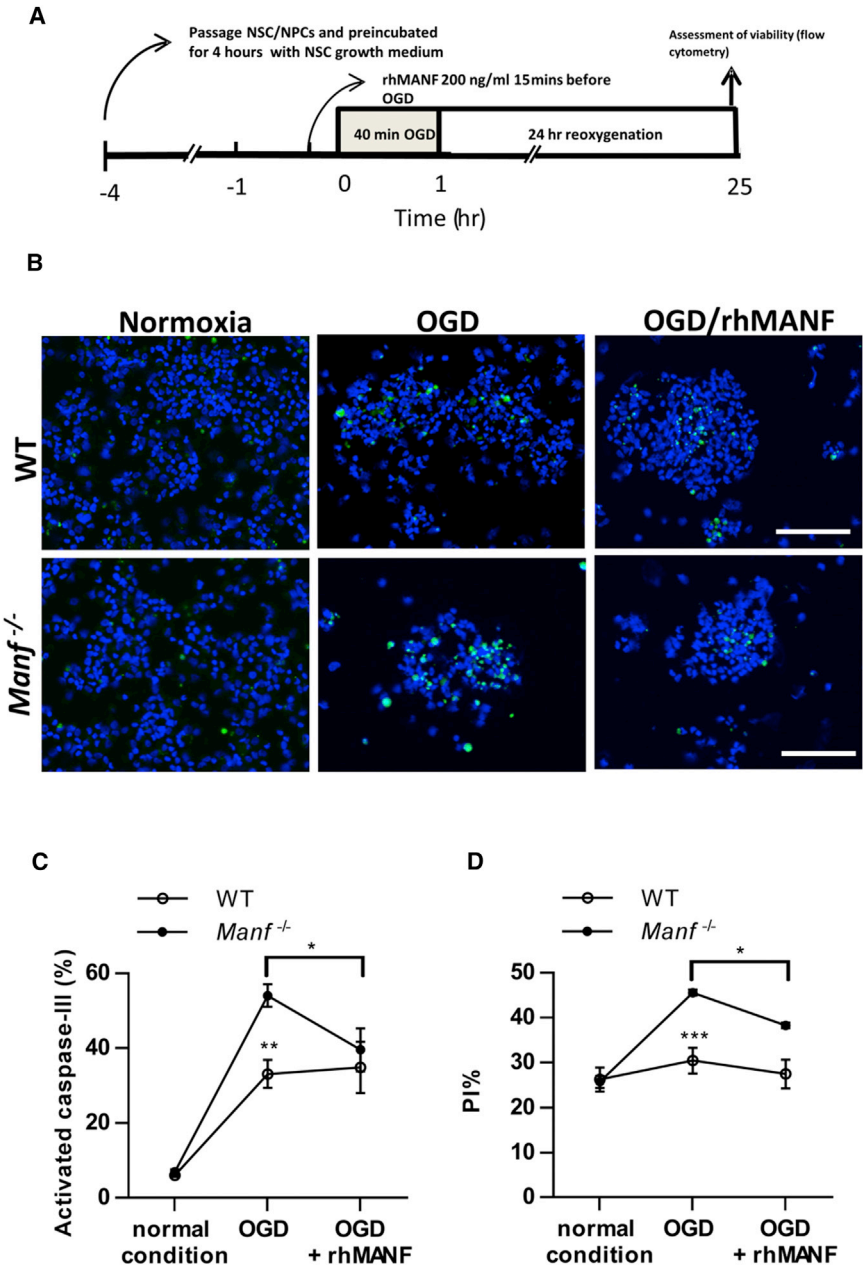

Figure 3. MANF Is Protective against OGD in NSCs

(A) Timeline of the oxygen-glucose-deprivation/reperfusion experiment. (B) Representative photomicrographs of activated caspase-3 labeling in the NSCs after OGD or under normal conditions. (C) Ratio of activated caspase-3+ cells in relation to $DAPI^+$ nuclei. Increase in activated caspase-3 density in $Manf^{-/-}$ cells after OGD treatment compared to WT cells. rhMANF treatment before OGD decreased activated caspase-3 density in $Manf^{-/-}$ cells (n = 6–11, two-way ANOVA, genotype X condition effect $p = 0.042$; $^{**}p < 0.01$ genotype effect; $^{*}p < 0.05$ $Manf^{-/-}$ OGD versus OGD + rhMANF). (D) Analysis of cell death by PI labeling. The percentage of PI^+ $Manf^{-/-}$ nuclei after OGD and reoxygenation was higher than in WT cells, indicating a greater apoptotic rate in $Manf^{-/-}$ cells. OGD-induced $Manf^{-/-}$ cell death was prevented by rhMANF treatment (n = 6 to 7, two-way ANOVA, genotype X condition effect $p = 0.001$; $^{***}p < 0.001$ genotype comparison; $^{*}p < 0.05$ $Manf^{-/-}$ OGD versus OGD + rhMANF). Scale bar, 100 μm (B). Data are presented as mean ± SEM.

Cultured SVZ explants were transduced with LV-hDCX-GFP (Figure 5F), LV-hDCX-myrAKT-GFP (Figure 5G), or LV-hDCX-hMANF-IRES-GFP (Figure 5H) on DIV1. Compared to control treatments, MANF overexpression enhanced the distance of cell migration at DIV6 (Figures 5F–5J). Moreover, MANF-overexpressing neuroblasts migrate in a chain-like form distal to the explants (Figure 5H, panel 2). Although high expression of myrAkt1 in DCX^+ cells increased the number of neuroblasts with pronounced neurite-like processes surrounding the SVZ explants, it did not noticeably increase the distance of cell migration from SVZ explants (Figures 5G, 5I, and 5J). These data suggest that stimulation of the Akt pathway may increase the number of neuroblasts but does not promote their migration. Contrarily, overexpression of MANF enhances the migration of neuroblasts from SVZ explants, probably by regulating signaling mechanisms other than the Akt-mTOR pathway in DCX^+ cells.

Overexpression of MANF Activates STAT3 and ERK1/2 during SVZ Cell Migration

Although a signal-transducing receptor for MANF has not been identified, MANF can exert its neurotrophic or neuroprotective effects through intracellular signals. Thus, we hypothesized that overexpression of MANF regulates molecular mechanisms involved in the migration of SVZ cells. We found increased levels of phosphorylated Akt (p-Akt) in SVZ explants after LV-hDCX-myrAKT-GFP transduction at DIV4 and DIV7 (Figures 6A–6C). Moreover, myrAKT significantly increased the levels of phosphorylated ribosomal protein S6 (p-S6K) at DIV4 and DIV7 (Figures 6D–6F), but did not stimulate ERK activation (Figures 6G–6I), indicating that myrAKT specifically activated the AKT/mTOR pathway. Conversely, overexpression of MANF did not increase p-AKT and p-S6K levels but significantly activated the p-ERK/ERK pathway on DIV4 (Figures 6G and 6I). However, there was no difference in the ratio of p-ERK1/2 to ERK1/2 between groups on DIV7 (Figures 6H and 6I), suggesting overexpressed MANF only increased phosphorylation of ERK1/2 at the beginning of cell migration. In line, overexpression of MANF also increased the level of p-STAT3-SER727

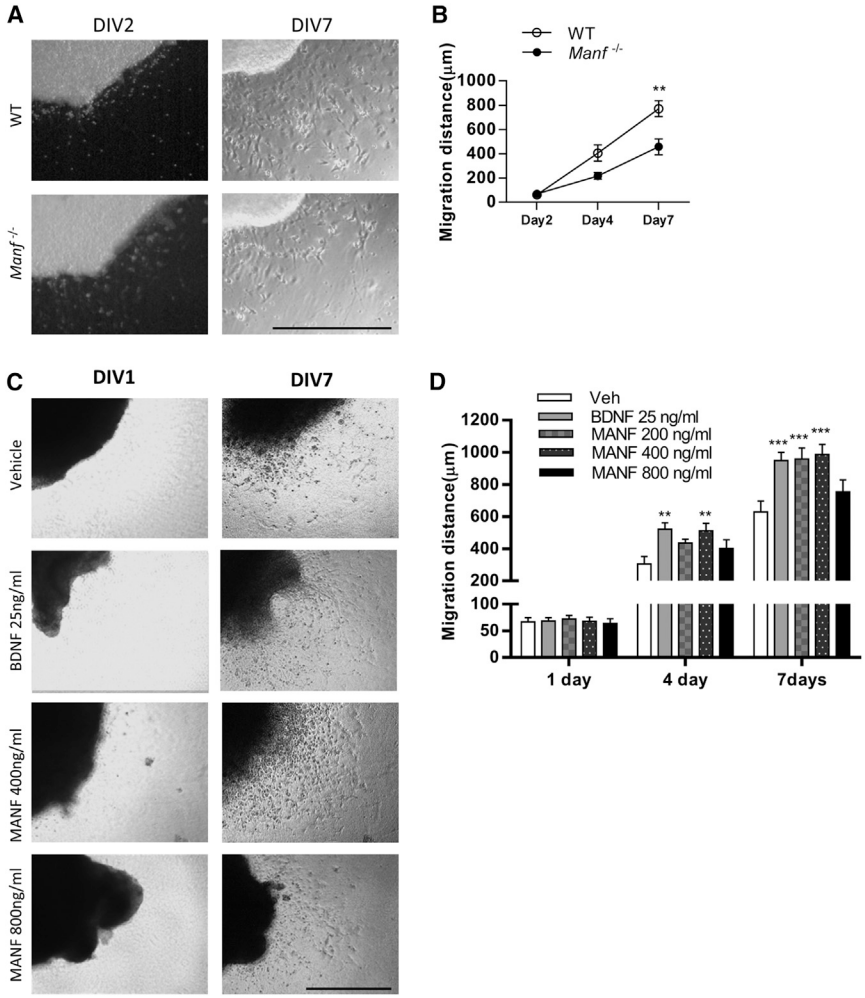

Figure 4. Effects of MANF on Cell Migration from the SVZ Explants

(A) Representative images of SVZ explants at DIV2 and DIV7 from WT and *Manf*$^{-/-}$ embryos. (B) MANF-deficient cells from the SVZ explants migrate shorter distances than WT cells at DIV7 (two-way ANOVA, genotype X time effect $p = 0.02$; $^{**}p < 0.01$ TK, n = 7 to 8). (C) 64 SVZ explants treated with rhMANF (0, 200, 400, and 800 ng/mL) or rhBDNF (25 ng/mL) from day 1 to day 4 and representative photomicrographs are shown from DIV1 and DIV7. (D) BDNF and MANF treatments significantly increased the migration of cells (n = 7 to 8, two-way ANOVA, treatment × time $p < 0.01$). At DIV4, the migration of cells was significantly increased from BDNF and rhMANF (400 ng/mL) treated SVZ explant ($^{**}p < 0.05$, TK). At DIV7, BDNF and rhMANF (200 and 400 ng/mL) treatments enhanced the distance of migration ($^{***}p < 0.001$ TK). Scale bars, 500 μm (A) and 1,000 μm (C). TK, Tukey's post hoc test. Data are presented as mean ± SEM.

at DIV4, and it returned to baseline levels at DIV7 (Figures 6J–6L). Although MANF has been implicated in regulating UPR markers, there was no difference in GRP78 protein levels between groups at any time points (Figures 6M–6O). Together, these results suggest that overexpressed MANF promotes migration of DCX$^+$ cells as well as regulates STAT3 and ERK1/2 activation.

DCX$^+$ Cells in SVZ, Neocortex, and Corpus Callosum after dMCAo

To clarify the pattern of neuroblast migration in the cortical stroke model, adult rats were sacrificed 2, 7, 14, and 28 (n = 4) days after dMCAo and the number of DCX$^+$ cells were quantified in the SVZ, corpus callosum, and infarction area (Figure S1A). We did not observe any DCX$^+$ cells in the neocortex in non-stroked rats. However, the dMCAo-lesioned rats exhibited increased numbers of DCX$^+$ cells in the ipsilateral SVZ from day 2 post-stroke (Figure S1B). On day 14 post-stroke, we found few DCX$^+$ cells in the infarcted neocortex composed of infarcted core and ischemic penumbra (Figure S1A). The DCX$^+$ cells in the infarcted area of neocortex had a morphology resembling that of differentiated post-migratory neurons with branched processes (Figure S1A, day 14, arrow). More DCX$^+$ cells were observed in the ipsilateral corpus callosum, and these cells exhibited a migratory morphology, with leading and trailing processes (Figure S1A, day 14, arrowhead). Quantification of DCX$^+$ cell numbers in the ipsilateral and contralateral SVZ, infarcted area of the neocortex, and corpus callosum beneath the infarction core revealed a significant increase in the number of DCX$^+$ cells in the ipsilateral SVZ on days 2, 7, 14, and 28 compared to the non-stroke group (Figure S1B). Moreover, the number of DCX$^+$ cells in the corpus callosum was highest on post-stroke day 14, implying that the number of neuroblasts observed in the corpus callosum beneath the infarction zone is time dependent.

MANF Did Not Affect NPC Proliferation in the SVZ but Promoted the Migration of DCX$^+$ Cells toward the Infarct Boundary

Stroke rats were stereotaxically injected with GDNF (n = 5), rhMANF (n = 6), or vehicle (n = 6) into their right (ipsilateral to stroke) lateral ventricles on days 3, 7, and 10 after dMCAo. BrdU was administered from days 3 to 10, and brains were collected on day 14 (Figure 7A). There was no difference in infarction size among the three groups (Figures 7B and 7C). As expected, GDNF treatment enhanced BrdU incorporation in the SVZ ipsilateral to the lesion (Figures 7D and 7E). The increased number of BrdU-labeled cells in the SVZ of GDNF-treated animals suggests increased cell proliferation. Immunoreactivity for DCX was examined in 17 stroke rats on day 14 post-stroke. GDNF treatment significantly increased the density of DCX immunoreactivity in the ipsilateral SVZ (Figures 7F and 7G). However, MANF treatment neither increased cell proliferation nor

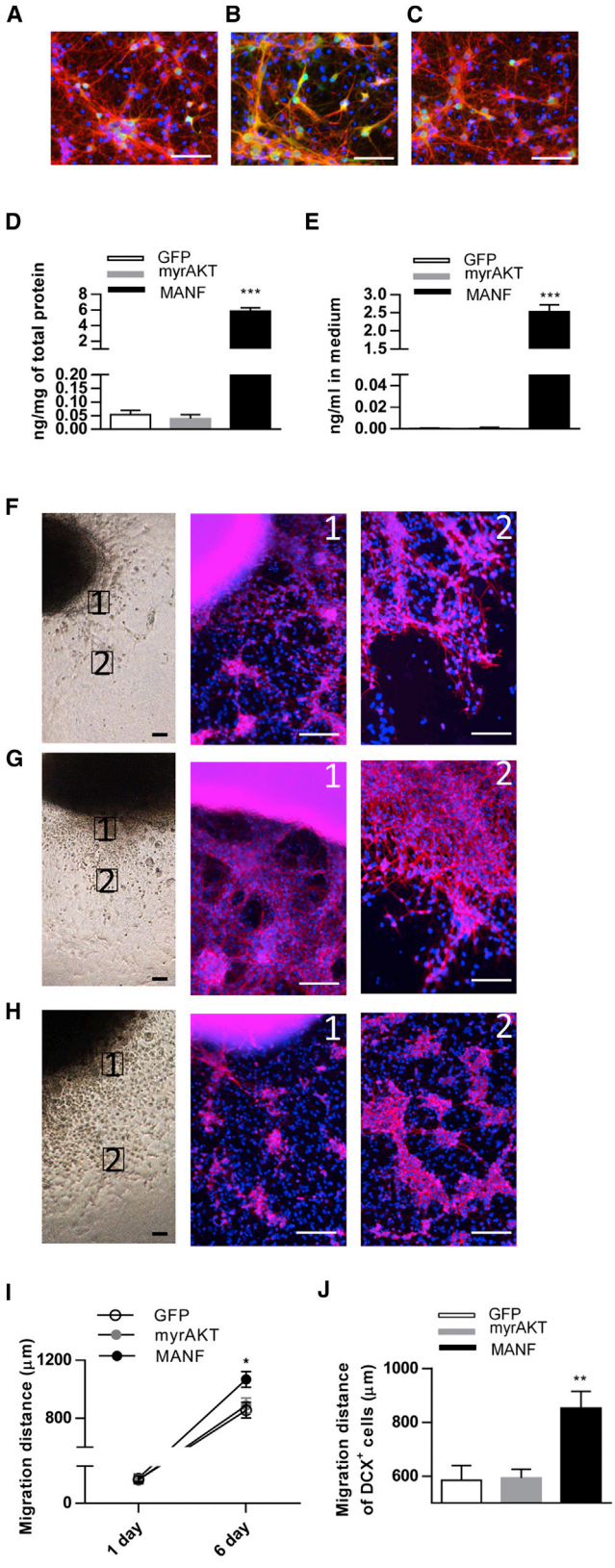

Figure 5. Transduction of SVZ cells with LV-MANF Enhances Cell Migration from SVZ Explants Derived from P1 Mouse Brain

(A–C) Embryonic cortical neurons transduced with LV-hDCX-GFP (A), LV-hDCX-myrAKT-GFP (B), and LV-hDCX-hMANF-IRES-GFP (C) after 5 days in culture. Photomicrographs show immunofluorescent labeling of neurons with anti-DCX (red), and anti-GFP (green) and counterstained with DAPI (blue). (D and E) MANF protein concentration in cell lysates (D, n = 5 to 6) and culture media (E, n = 3 to 4) from embryonic cortical neurons transduced with indicated LVs (one-way ANOVA $p < 0.001$, ***$p < 0.001$ compared to GFP, TK). (F–H) Representative photomicrographs of SVZ explants on the left. Panels 1 and 2 show immunostaining for DCX (red) and counterstaining with DAPI (blue) in the migrating cells from SVZ explants. The proximal (F1) and distal (F2) area of migrating DCX^+ cells transduced with LV-GFP (F). (G) Representative images of myrAKT-expressed SVZ explants. (G1) The density of DCX-stained cells close to SVZ explants was increased when compared to GFP controls. (G2) High density of migrating DCX^+ cells distal to SVZ explants. (H) Representative photomicrographs of LV-MANF-treated SVZ explants. (H1) Immunofluorescent staining of DCX^+ cells close to SVZ explants. (H2) Overexpression of MANF in SVZ resulted in chains of neuroblasts, which migrated further from explants at DIV6 compared to controls. (I) Quantified migration distance at DIV1 in all groups (n = 4 to 5) and at DIV6 revealed increased cell migration from SVZ explants transduced with LV-MANF as compared to the GFP group (n = 11 to 12, one-way ANOVA $p = 0.02$; *$p < 0.05$ TK). (J) Quantification of migratory distance of cells from SVZ explants. MANF increased the migratory distance of cells migrating from SVZ explants (n = 18–22, one-way ANOVA $p = 0.0005$, **$p < 0.01$ compared to GFP and myrAKT, TK). Scale bars, 50 μm (A–C) and 100 μm (F–H). TK, Tukey's post hoc test. Data are presented as mean ± SEM.

the number of DCX^+ cells in the SVZ compared to the vehicle group, suggesting that MANF injections did not enhance the dMCAo-induced proliferative response.[36] Next, we quantified the number of neuroblasts by counting DCX^+ cells in different areas. GDNF markedly increased the number of DCX^+ cells in the ipsilateral striatum and induced more chains of neuroblasts with long processes. MANF also increased the number of DCX^+ cells in the ipsilateral striatum but did not influence their morphology (Figures 7H and 7I). Additionally, we examined the number of DCX^+ cells in the infarcted area of the neocortex and corpus callosum beneath the infarction zone. Surprisingly, GDNF did not increase the number of DCX^+ cells within the infarct boundary on day 14 after dMCAo (Figures 7J and 7K). Notably, compared to vehicle-treated and GDNF-treated rats, MANF significantly increased the number of DCX^+ cells in the corpus callosum and infarcted neocortex (Figures 7J–7M). Moreover, MANF induced recruitment of robust chains of neuroblasts in the corpus callosum beneath the infarction zone and promoted more neuroblasts with long, branched processes in the infarcted neocortex. Taken together, these data reveal that administration of MANF into the right lateral ventricle facilitates migration of the NPCs to the injured cortex.

We next explored whether MANF, compared to GDNF, influences the fate of newly generated cells 14 days after 90 min dMCAo. MANF treatment markedly increased the number of cells labeled with BrdU and DCX in the corpus callosum beneath the infarction zone compared to vehicle and the GDNF-treated group (Figures 8A and 8B). There was a trend toward fewer cells double labeled with BrdU and the astrocyte marker GFAP in the infarcted area of the neocortex in the MANF and GDNF treatment groups (Figures 8C

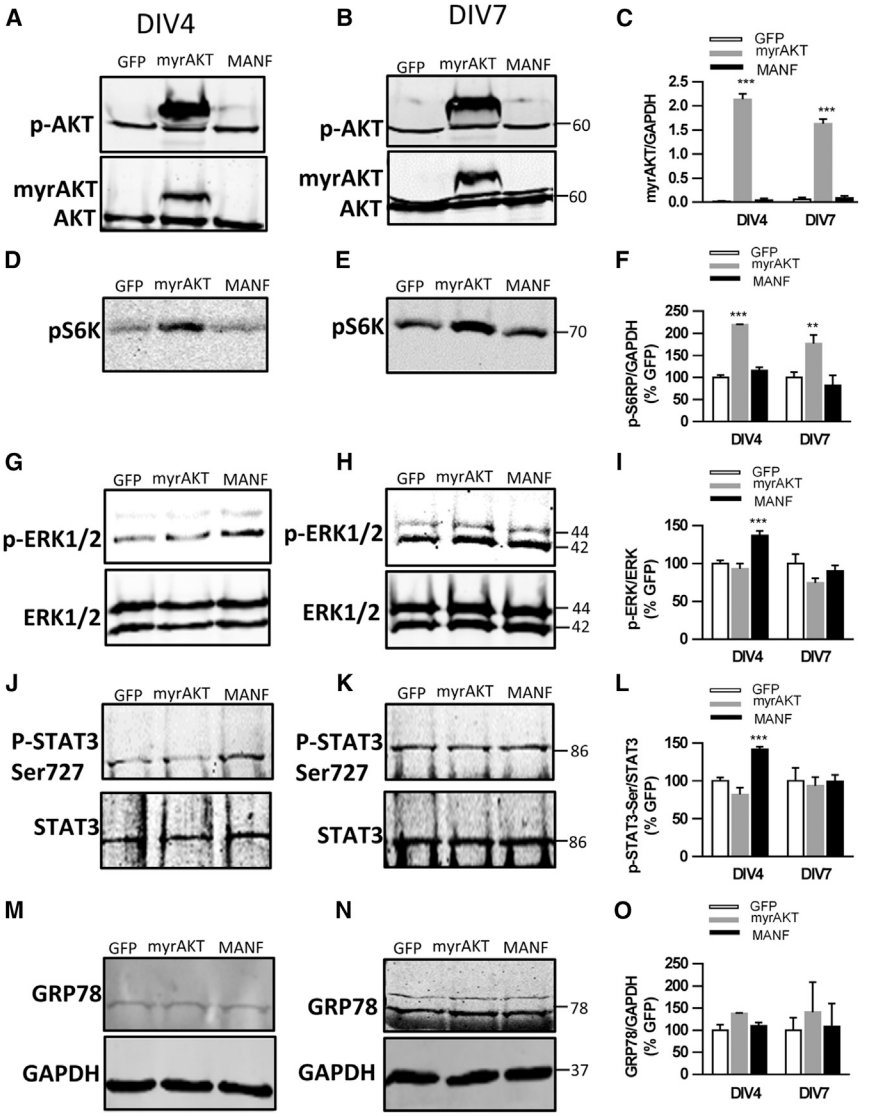

Figure 6. Overexpression of MANF Activates ERK1/2 and STAT3 Signaling in the SVZ Explant Culture

SVZ explants were transduced with LV on DIV1 and analyzed using western blotting at DIV4 or DIV7. (A and B) The expression of myrAKT at DIV4 (A) and DIV7 (B) were detected in LV-myrAKT-transduced SVZ explants. (C) Quantitated level of myrAKT relative to GAPDH (n = 3, two-way ANOVA, time × LV treatment, $p < 0.01$, $^{***}p < 0.001$ compared to GFP, TK). (D and E) Increased expressions of phospho-S6K (P-S6K) was detected at DIV4 (D) and DIV7 (E) in LV-myrAKT-treated SVZ explants. (F) Quantification of P-S6K level relative to GAPDH and increased levels were observed in LV-myrAKT-treated explants (two-way ANOVA, treatment effect $p < 0.001$, $^{**}p < 0.01$, $^{***}p < 0.001$ compared to GFP TK). (G and H) Increased expression of p-ERK1/2 in MANF-overexpressed SVZ explants at DIV4 (G), but not at DIV7 (H). (I) Quantified expression levels of p-ERK compared to total ERK showed statistically significant elevated levels of p-ERK in LV-MANF at DIV4 compared to LV-GFP and LV-myrAKT groups (two-way ANOVA, $p < 0.05$, $^{***}p < 0.01$, TK) but not at DIV7. (J and K) Overexpression of MANF induced p-STAT3-Ser in SVZ explants at DIV4 (J), but not at DIV7 (K). (L) Statistically significant elevated levels of p-STAT3-Ser in LV-MANF at DIV4 compared to LV-GFP and LV-myrAKT groups (two-way ANOVA, $p < 0.05$, $^{***}p < 0.001$, TK), but not at DIV7. (M–O) There was a modest expression of the UPR-regulated protein GRP78 at DIV4 (M) and DIV7 (N), and it did not differ between groups at either time point (O). TK, Tukey's post hoc test. Data are presented as mean ± SEM.

and 8D). Meanwhile, the number of $BrdU^+$ cells co-expressing the oligoprogenitor cell marker NG2 was not different among the three groups (Figures 8E and 8F). Thus, the administration of MANF after cortical stroke may have selectively affected the migrating immature cells of the neuronal lineage.

Long-term Infusion of MANF Increased Recruitment of DCX^+ Cells in Infarct Cortex

We tested whether long-term infusion of MANF increases the number of newborn neurons in the lesioned cortex. Using osmotic minipumps, GDNF, MANF, or vehicle were infused into the peri-infarction zone for post-dMCAo days 3–16 and the rats were euthanized 1 week later (Figure 9A). Lesion size did not differ among the three groups (Figures 9B and 9C). GDNF infusion resulted in a trend of increasing numbers of DCX^+ cells in the right SVZ and corpus callosum on day 24 after stroke (Figures 9D–9G), suggesting that GDNF infusion into the peri-infarction zone might enhance stroke-induced neurogenesis in the ipsilateral SVZ. In contrast to GDNF, MANF infusion did not increase the number of DCX^+ cells in the SVZ nor in the corpus callosum. Importantly, we observed that GDNF and MANF treatments increased the number of DCX^+ cells in the infarct area of the neocortex (Figures 9H and 9I). These results suggest that GDNF, a classical chemoattractant, increases the number of NPCs close to where it is administered. However, MANF seems to directly enhance migration of neuroblasts toward the lesioned cortex.

We continued to explore whether MANF or GDNF promotes neuronal maturation of the NPCs in the lesioned cortex by using double-label immunofluorescence. Stroke rats treated with long-term infusion with GDNF (n = 5), MANF (n = 5), or vehicle (n = 5) were injected with BrdU and sacrificed on day 24 after dMCAo. Epifluorescent microscopic examination indicated that few $BrdU^+$ cells in the lesioned cerebral cortex expressed the post-mitotic neuronal markers NeuN and MAP2. Due to the diffuse staining pattern of MAP2, it was difficult to determine the co-localization of BrdU and MAP2 (data not shown). There was a marginal

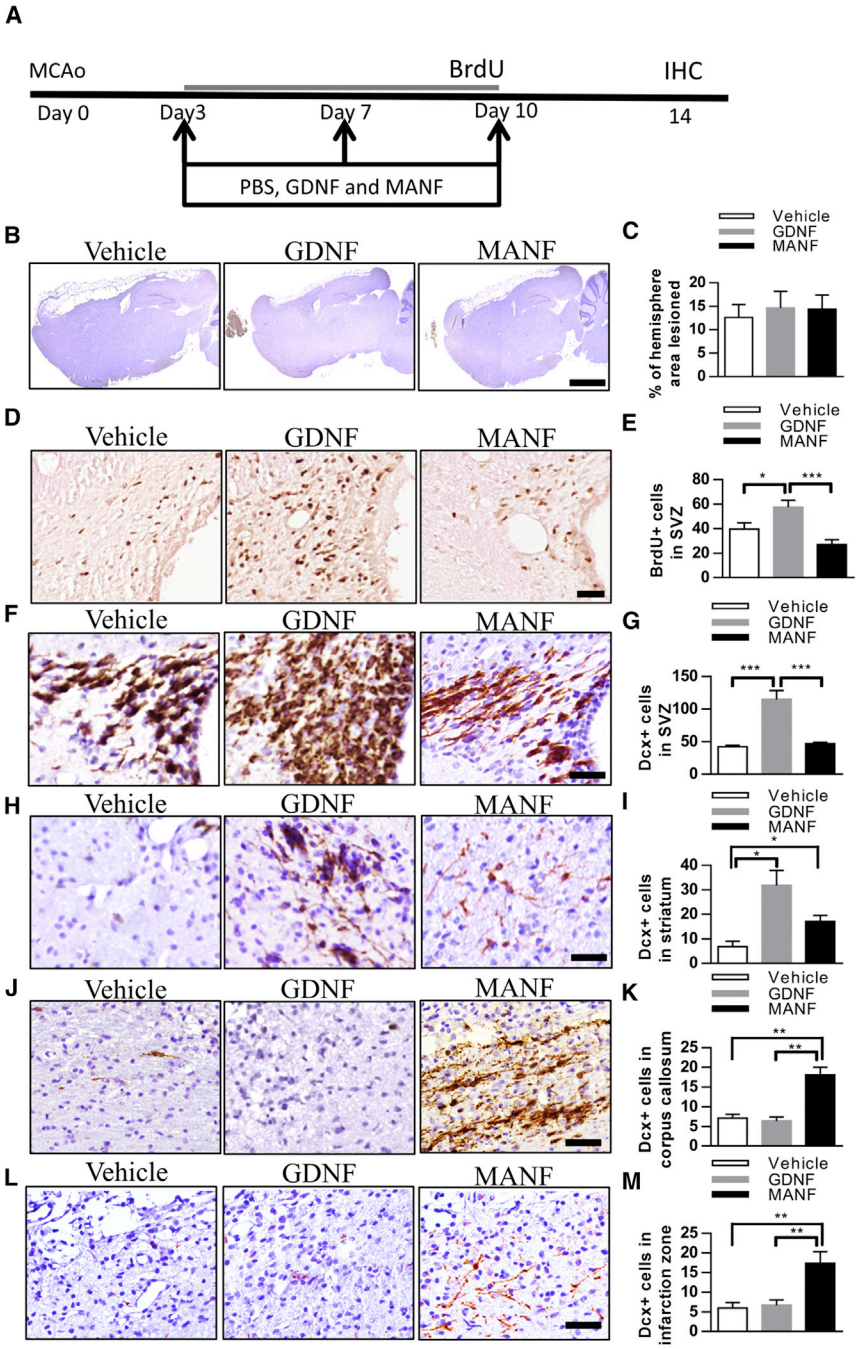

Figure 7. Post-stroke Treatment with GDNF Enhances Neurogenesis in the SVZ, but MANF Promotes Migration of DCX⁺ Cells toward the Infarction Area

(A) Timeline of treatment. (B) Representative photomicrographs of infarction areas in different groups. (C) Infarction area was similar between groups. Nissl^{-} area expressed as % of the whole area of the hemisphere. (D) Representative photomicrographs of BrdU immunoreactivity in the SVZ. (E) The number of BrdU-stained cells was increased in ipsilateral SVZ of stroke rats receiving three intraventricular injections of GDNF compared to vehicle or MANF treated (dose of 10 μg, n = 5 to 6, one-way ANOVA $p < 0.01$, *$p < 0.05$, ***$p < 0.001$ LSD. (F) Representative photomicrographs of DCX immunoreactivity in the SVZ. (G) GDNF injections increased DCX⁺ immunoreactivity in the right SVZ compared to the MANF- or vehicle-treated groups by almost 3-fold (one-way ANOVA $p < 0.001$, ***$p < 0.001$ TK). (H) Representative photomicrographs of DCX immunoreactivity in the striatum. (I) GDNF or MANF injections increased the recruitment of neuroblasts (DCX⁺ cells) into the striatum after stroke compared to vehicle by 4- and 2-fold, respectively (one-way ANOVA $p < 0.05$, *$p < 0.05$ TK). (J and L) Representative photomicrographs of DCX immunoreactivity in the corpus callosum (J) and infarction zone (L). (K and M) MANF promoted the migration of DCX⁺ cells toward the right corpus callosum by 3-fold (K; one-way ANOVA $p < 0.001$, **$p < 0.01$ TK) and the infarct area of the neocortex by 3-fold (M; one-way ANOVA $p < 0.01$, **$p < 0.01$ TK). No effect was observed with GDNF. Scale bars, 2,000 μm (B) and 50 μm (D–L). LSD, Fisher's LSD post hoc test; TK, Tukey's post hoc test. Data are presented as mean ± SEM.

increase in NeuN/BrdU density after MANF administration (Figures 9J and 9K).

DISCUSSION

We are the first to demonstrate that MANF is robustly expressed in adult SVZ cells. Loss of MANF does not affect self-renewal or viability of NSCs in vitro. However, *Manf*$^{-/-}$ NSCs are more vulnerable to OGD- and reoxygenation-induced cell injury, and treatment with MANF protein rescues apoptotic *Manf*$^{-/-}$ cells. Although the extracellular application of MANF had no mitogenic effect, it induced the differentiation of NSCs, accompanied by increased levels of neuron-specific tubulin and glial-associated cytoskeleton protein as well as activation of the STAT3 pathway. Additionally, endogenous and exogenous MANF stimulated cell migration from SVZ explants. Overexpression of endogenous MANF activated not only STAT3 but also the ERK1/2 pathway at the beginning of cell migration. In the cortical ischemic-reperfusion injury experiments, intracerebroventricular MANF injections promoted neuroblast migration toward the infarct boundary on day 14 post-stroke. Furthermore, long-term infusion of MANF into the peri-infarction zone increases the recruitment of neuroblasts within the infarction area in the neocortex on day 24 post-stroke.

Our previous studies have shown that in neurons in vitro, MANF is neuroprotective when it is expressed inside the cell.[33,37] Moreover, a recent study showed that in order to be neuroprotective

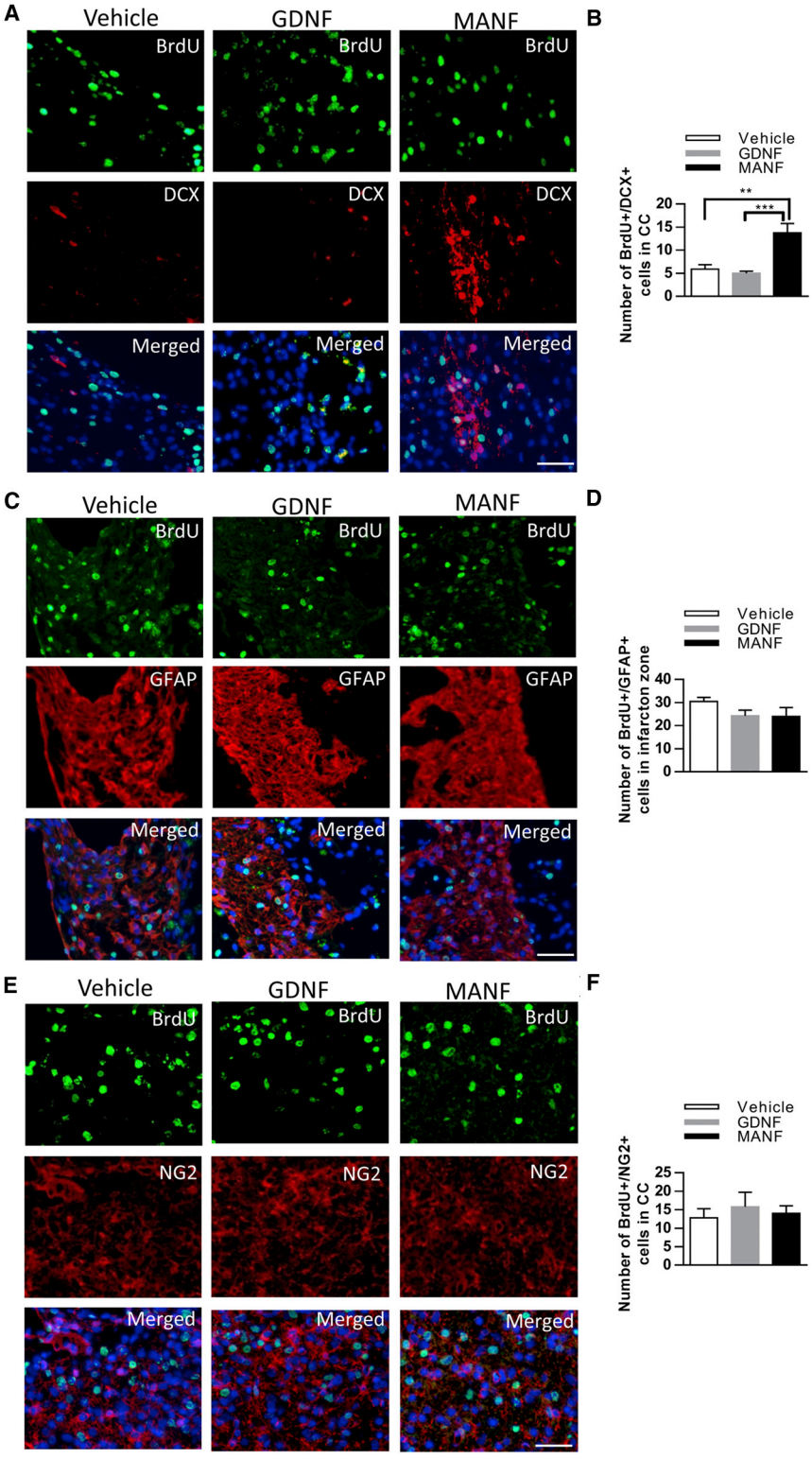

Figure 8. MANF Injections, 3 × 10 μg, Resulted in Increased Numbers of Neuroblasts in the Corpus Callosum after Stroke

(A) Distribution of $DCX^+/BrdU^+$ cells in the corpus callosum beneath the infarction zone. (B) Number of $DCX^+/BrdU^+$ cells in the ipsilateral corpus callosum increased due to MANF treatment ($n = 5$ in all groups, one-way ANOVA $p < 0.001$, $^{**}p < 0.01$, $^{***}p < 0.001$ TK). (C) GFAP immunostaining showed that most BrdU-labeled cells also express GFAP in the infarction zone. (D) The number of $GFAP^+/BrdU^+$ cells in the infarction zone did not differ between groups. (E) $NG2^+$ cells expressing BrdU within the infarct boundary. (F) Number of $BrdU^+/NG2^+$ cells in the corpus callosum beneath the infarction zone did not differ between treatment groups; scale bars, 50 μm. Data are presented as mean ± SEM.

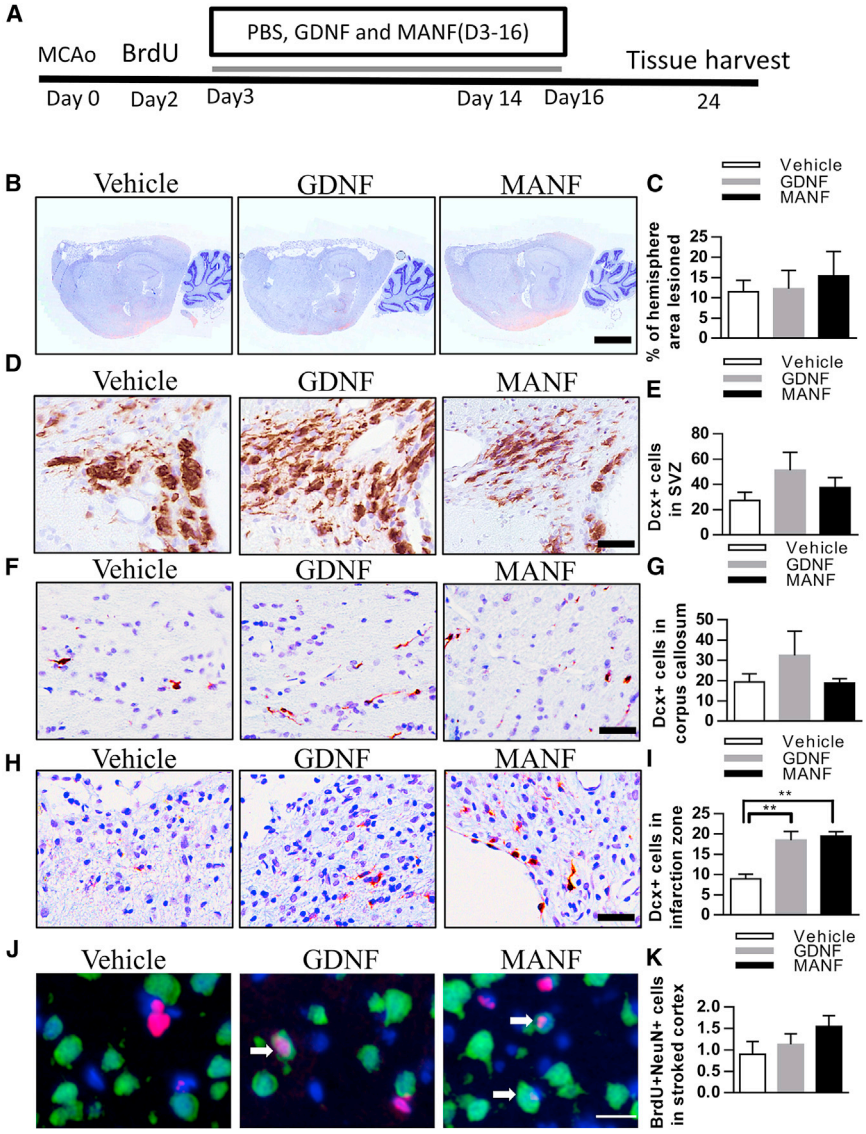

Figure 9. Effect of Long-Term GDNF and MANF, 0.25 μg/μL, a total of 200 μL, Infusion in the Peri-infarction Zone after Cortical Stroke

(A) A timeline of the experiment. (B) Representative photomicrographs of infarction areas in different groups. (C) Staining and quantification of lesioned brain areas show similar infarction sizes between groups, n = 5. (D–H) DCX^+ cells after PBS, GDNF, or MANF administration in the SVZ (D and E), corpus callosum (F and G), and infraction zone (H). (I) GDNF and MANF treatments increase the number of DCX^+ cells in the infarction zone (n = 4 to 5, one-way ANOVA $p < 0.01$, $^{**}p < 0.01$ TK). (J) Images of NeuN (green) and BrdU (red) double-labeled cells in the peri-infarction zone. (K) A trend toward increase in the number of new mature cortical neurons in the peri-infarction zone with MANF treatment. n = 5. Scale bars, 2,000 μL (B), 50 μm (D–H), and 20 μm (J). Data are presented as mean ± SEM.

in vitro MANF needs to be localized within the ER.[37] Although previous in vitro studies have shown that extracellular MANF administration also has neuroprotective effects,[38] the specific receptor that MANF binds to on the plasma membrance was still obscure.[33] In this study, we examined the effects of MANF on NSCs by deletion of *Manf* gene expression or administration of exogenous MANF into the culture medium. We demonstrated increased vulnerability of MANF-deficient NSCs to OGD- and reoxygenation-induced stress and that administration of exogenous rhMANF only rescued cells lacking MANF. However, exogenously administered MANF protein did not show a protective effect for WT cells, suggesting MANF plays a cell-autonomous role in NSC survival from stress. Furthermore, these findings suggest that endogenous MANF plays a crucial role for NSC survival in OGD and reoxygenation stress. Additionally, we postulated that endogenous MANF could be secreted from WT NSCs after OGD and reoxygenation injury and that the protective effect may be exerted by MANF released from the injured cells, masking the protective effect of exogenously added MANF in the medium. A possible autocrine or paracrine mechanism could also explain why MANF-deficient NSCs are more vulnerable to stress than WT cells and therefore responsive to rhMANF treatment.

MANF has been implicated as a neurotrophic factor,[39] and in the fruit fly, is necessary for the maturation of dopaminergic neurons.[40] However, our data suggest a more extensive regenerative role for MANF in the mammalian brain. Because MANF is expressed in proliferating NSCs, we initially hypothesized that MANF might be implicated in the regulation of NSCs proliferation. However, the size and self-renewal of neurospheres were not affected by MANF removal or exogenous administration in cultured NSCs. MANF did not affect the number of $BrdU^+$ cells after cortical ischemic injury, a state in which NSC proliferation in the brain is induced. Thus, MANF seems to be dispensable in the regulation of NSC proliferation. In particular, because MANF did not affect proliferation of SVZ cells after stroke, it could be an advantage for possible clinical use of MANF because some growth factors could induce dysplastic and phenotypical changes by stimulating uncontrolled cell proliferation.[41,42]

The signaling pathways activated by MANF are still largely unclear. Recently, a study has shown that the administration at concentrations higher than 1 μg/mL of rhMANF increased protein kinase C (PKC) phosphorylation in a time-dependent manner.[43] PKC has multiple

subtypes and the subtypes have different effects; for example, PKCδ increases the activity of STAT3 and PKCɣ triggers ERK1/2 activation.[44,45] We found that rhMANF treatment (400 ng/mL) activates the STAT3 pathway during the process of neuronal and glial differentiation of NSCs. STAT3 is a classic transcription regulator, which was first discovered as a key mediator of cytokine-induced inflammation and immunity.[46] Later studies have found STAT3 to regulate a wide range of biological processes, including determining the fate of NSCs.[47,48] Many studies have reported that GFAP expression in NPCs is dependent on the activation of STAT3 and its phosphorylation at Tyr705.[49–51] Thus, STAT3 activation could be crucial for astrocyte differentiation. Also, it has been suggested that STAT3 is involved in neuronal differentiation and it regulates neuron-specific microtubules by antagonizing the depolymerization activity of stathmin.[52] Importantly, serine-phosphorylated STAT3 localized to the mitochondria instead of the nucleus is involved in neurite outgrowth induced by nerve growth factor (NGF).[53] In this study, we found that STAT3 phosphorylation on Tyr705 and Ser727 is induced following MANF treatment in primary NSCs. These findings led us to assume that MANF could promote neuronal and glial differentiation via activation of STAT3 pathway. Although we did no further investigation of whether inhibition of STAT3 signaling blocks the NSC differentiation-promoting effect of exogenous MANF, the identification of NSCs as a target for MANF in our study may accelerate to clarify the MANF-mediated signaling pathways. Meanwhile, exogenous MANF did not activate ERK1/2 pathway in NSCs, which has been suggested to be involved in Ser727 phosphorylation of STAT3,[54] and the reason for this remains to be explored. Further studies will be required to determine the putative MANF receptors on NSCs and the mechanistic link between MANF and the STAT3 signaling pathway.

Next, we showed that MANF has a role in NPC migration. LV-mediated overexpression or extracellular administration of MANF enhances migration of cells from the SVZ explants, whereas lack of MANF reduced it. In line with the effect of rhMANF on NSCs, overexpressed MANF induced activation of STAT3 during SVZ cell migration. Surprisingly, it also activated the ERK1/2 pathway at DIV4. The ERK1/2 pathway regulates the differentiation of NSCs through a number of mechanisms[55–57] and is implicated in cell migration induced by growth factors.[58] On the other hand, inhibition of ERK activity has been shown to impair cell migration stimulated by different growth factors, including vascular endothelial growth factor (VEGF), epidermal growth factor (EGF), and fibroblast growth factor (FGF).[59] Although the overexpression of MANF causes ERK1/2 phosphorylation in SVZ explants, we do not know whether this activation was directly induced by MANF or STAT3-related downstream targets. Because phosphorylated and activated STAT3 upregulates expression of genes encoding for growth factors such as VEGF or HIF1α in many cell types,[60] we assumed that the ability of MANF to induce STAT3 activation can trigger neuronal and glial differentiation preceding cell migration. However, it is also possible that STAT3 activation by MANF increases the expression levels of growth factors, which thereby activate cell membrane receptors and downstream ERK1/2 signaling pathways, leading to increased cell migration.

Cerebral ischemia can trigger endogenous repair processes and activate proliferation of NSCs. However, most of these cells die and do not migrate to the lesioned area.[7] GDNF has been shown to enhance NSC proliferation in the SVZ and NPC recruitment to the ischemic lesion.[18] In this study, we observed that intraventricular injections of GDNF increased cell proliferation in the SVZ, but not the number of NPCs in the infarct boundary on day 14 post-stroke. There are several possible explanations for this discrepancy. First, we utilized a dMCAo model that restricts ischemic lesions mainly to the neocortex without affecting the striatum. Meanwhile, Kobayashi and coworkers[18] used an intraluminal filament technique to generate infarction in a broad brain area, including the striatum, and therefore, increased NPC recruitment could have been caused by damage occurring closer to the SVZ. Second, the GDNF infusion sites were different. In our study, GDNF was infused into the lateral ventricle, whereas Kobayashi and coworkers[18] infused GDNF intra-striatally so that GDNF diffused throughout the striatum, including the SVZ. This could demonstrate that recruitment of neuroblasts to the infarcted striatum may be due to the chemoattractant effect of GDNF or secondarily due to the increased numbers of NPCs in the SVZ. Previous studies have shown that compared to GDNF, MANF diffuses in the brain significantly better.[34] Therefore, the increased migration of NPCs from the SVZ toward the infarct area of the neocortex could be attributable to a better distribution of MANF in brain tissue. Particularly, we also found that in sham surgery rats treated with MANF, there were no DCX^+ cells moving to intact cortex or only few DCX^+ cells in the striatum, similar to the PBS group. Contrarily, GDNF administration seemed to cause more DCX^+ cells in the striatum in the sham rats (data not shown), suggesting that GDNF exerts chemoattractant effects to guide migration of the cells in the SVZ. Moreover, MANF may have a direct effect on NPC motility or improve the microenvironment in the lesioned area to improve NPC migration.

Finally, we compared the effects of long-term local infusion of MANF and GDNF into the peri-infarct region on the number of DCX^+ cells in the infarct area. In contrast to vehicle controls, local infusions of MANF and GDNF increased the number of DCX^+ cells in the infarct cortex on day 24 post-stroke by 2-fold. However, neither MANF nor GDNF significantly increased the number of newly generated neurons in the peri-infarct zone, implying that the migrating NPCs did not further differentiate to mature neurons. In our study, the infusion of MANF or GDNF continued for up to 16 days, similar to the temporal pattern of ischemia-induced neurogenesis and neuroblast migration described before.[9] Although we have also found that post-stroke MANF administration can induce behavioral improvement (K. Mätlik, J.E.A., K.Y. Tseng, O.P. Smolander, E. Pakarinen, L. Lehtonen, U. Abo-Ramadan, P. Lindholm, C. Zheng, B.K. Harvey, U. Arumäe, M.L., and M.A., unpublished results), MANF treatment did not accelerate neuronal maturation, which might occur at later time points. Therefore, the MANF-induced behavioral recovery is

not attributed to replacement of newly born neurons in the lesioned cortex. We hypothesize that this beneficial behavioral effect in stroke rats may be due to the ability of MANF to improve a microenvironment also supportive of migrating neuroblasts in lesioned sites; however, we cannot exclude involvement of other mechanisms to boost functional recovery. A recent report showed that MANF, exerting immunomodulation, improves the success of cell-replacement regenerative therapies in the retina[30] and the MANF paralog CDNF has an anti-inflammatory function in nerve regeneration after spinal cord injury.[61] Because post-stroke inflammation has been implicated in neuroblast migration[2,62] and stroke-induced behavioral deficit,[63] it is also possible that MANF could exert immune modulation to both recruit neuroblasts toward the stroked cortex as well as to hasten behavioral recovery.[64–66]

In conclusion, our results demonstrate that MANF treatment induces differentiation of NSCs and increases cell migration from SVZ explants, preceded by activation of STAT3. Also, this is the first study to demonstrate the neuroregenerative potential of MANF via promoting neuroblast recruitment to the lesioned cortex in stroke rats. MANF, distinct to GDNF, did not act as a classical growth factor, which increases proliferation of SVZ cells. However, it promoted migration of DCX^+ cells into the damaged cortex. Taken together, this study determines the effect of MANF in promoting the migration of NPCs in vivo and in vitro and suggests MANF to improve the effectiveness of stem-cell-based therapies for a damaged central nervous system.

MATERIALS AND METHODS

Isolation and Culturing of *Manf*$^{-/-}$ and WT NSCs

NSCs were prepared as previously described.[67,68] Briefly, the telencephalons along with the lateral ventricle of E14.5 WT (*Manf*$^{+/+}$) and *Manf*$^{-/-}$ mice were isolated and dissociated cells were cultured in NSC growth medium containing DMEM/F12 (Gibco) supplemented with B27 (20 μL/mL, Gibco), EGF (20 ng/mL, Gibco), FGF-2 (20 ng/mL, Gibco), GlutaMAX (10 μL/mL, Gibco), and penicillin-streptomycin (50 U/mL, Gibco). After 5–7 days of culture, neurospheres were dissociated by trituration and digestion (Accutase, Gibco). Neurospheres were passaged every 7–10 days.

OGD of Cultured Cells

We used previously described experimental procedures.[69] Briefly, NSCs and NPCs were passaged and 2.5×10^5 cells were pre-incubated for 4 hr in the growth medium. At first, we examined the viability of WT and mutant NSCs and NPCs in the normal condition (20% O2; 5% CO2 and 74% N2) and this was considered as the control group. Then, the medium was replaced with a deoxygenated glucose-free balanced salt solution (gfBSS) containing 120 mM NaCl, 5 mM KCl, 1.25 mM NaH_2PO_4, 2 mM $MgSO_4$, 25 mM $NaHCO_3$, 20 mM HEPES, and 2 mM $CaCl_2$. WT and *Manf*$^{-/-}$ cells were incubated in a hypoxic chamber (1% O_2; remainder 5% CO_2 and 94% N_2) for 40 min and re-incubated in neurosphere medium for 24 hr. To examine the effects of exogenous MANF on cells, rhMANF (200 ng/mL) was administered 15 min before 40 min OGD followed by 24 hr reoxygenation.

Analysis of Cell Death with PI Staining and Flow Cytometry

To analyze cell death and apoptosis of NSCs and NPCs following OGD, the cells were suspended into single cells by Accutase treatment, fixed with ice-cold 75% ethanol in PBS, and stained with 50 mg/mL PI (P5264, Sigma) for 5 min at 37°C. The cells were analyzed with a Gallios flow cytometer (Beckman Coulter), and data were analyzed using the Kaluza Flow Analysis 1.3 software (Beckman Coulter). The apoptotic rate was calculated as the ratio of PI^+ cells to the total number of NSCs.[70]

Recombinant Proteins

rhMANF was produced in CHO cells (Icosagen, Tallinn, Estonia); recombinant human GDNF (rhGDNF) or recombinant human BDNF (rhBDNF) was purchased from ProSpec-Tany TechnoGene (Rehovot, Israel) and R&D Systems (248-BD), respectively.

Construction of Transfer Plasmids and Production of Lentiviral Vectors

A 2.2 kb fragment of human DCX promoter was PCR amplified using Phusion high fidelity DNA polymerase (Thermo Scientific) and the following primers, BcuI_hDcx_for 5′-ATACTAGTGGATACTT GAGCTAAACTGCCT and EcoRI_hDcx_rev 5′-TTGAATTCCCT CAGAGACCTGA, digested with FastDigest-BcuI/-EcoRI (Thermo Scientific), cloned into the pCDH-CMV-MSC-T2A-EGFP vector (System Biosciences), and redigested with the same restriction enzymes. To obtain the pCDH-hDCX-IRES-GFP vector, the IRES-GFP fragment was released from the pMX-IRES-GFP vector[71] by digestion with FastDigest-NotI/-SalI (Thermo Scientific), cloned into the pCDH-hDCX-MSC-T2A-EGFP backbone, and redigested with the same enzymes. Coding sequences of hMANF were PCR amplified from human tissue cDNA with the following primers, MANF_For 5′ AATTTAAATCGGATCCACCATGTGGGCCACG CAG, MANF_Rev TAGCGGCCGCGGATCCTACAAATCGGTCC GTGCACTG, and cloned into a pCDH-hDCX-IRES-GFP vector digested with FastDigest-BamHI (Thermo Scientific) using In-Fusion cloning (Clontech) to obtain pCDH-hDCX-hMANF-IRES-GFP lentiviral transfer plasmids. Myristoylated constitutively active Akt1 (myrAkt) cDNA (Merck, #21-151) was cloned into the FastDigest-EcoRI/-NotI-digested pCDH-hDCX-T2A-GFP vector. All plasmid constructs were verified by DNA sequencing.

Lentiviral vectors (LVs) were produced as described,[72–74] with the following modifications. Briefly, human HEK293T cells (ATCC #CRL-1573) grown on 10-cm cell culture dishes in DMEM (Gibco) with 10% fetal bovine serum (Gibco) and 1 mg/mL normocin (InvivoGen) were transfected using linear polyethylenimine (Polysciences, #23966-2) with 10 μg transfer plasmid and 5 μg each helper plasmids (pMDLg/pRRE, Addgene, #12251; pRSV/REV, Addgene, #12253; and pMD2.G Addgene, #12259). At 5 to 6 hr post-transfection, the medium was changed to that containing 25 mM HEPES, pH 7.4. After 60 hr, supernatants were

collected, filtered, centrifuged, and re-suspended in Dulbecco's PBS (Gibco).

Primary Embryonic Cortical Neuron Cultures

Neocortical tissue from E16 embryos of timed, pregnant mice were used to prepare neuronal cultures as described.[75] Cells (7×10^4 viable cells/well) were cultured in Neurobasal medium (Life Technologies) supplemented with B27 (Life Technologies), 300 μM glutamine (Life Technologies), and streptomycin and amphotericin B (Life Technologies) and plated in 96-well plates coated with poly-D-lysine. Cells were transduced with LV-hDCX-GFP, LV-hDCX-myrAkt-GFP, or LV-hDCX-hMANF-IRES-GFP, respectively, on DIV1 using MOI of 5. Cells were fed by 50% media exchange on DIV3. On DIV5, the cells were fixed with 4% paraformaldehyde (PFA) for 15 min and immunostained.

ELISA for hMANF

hMANF protein levels were analyzed with an in-house-built sandwich ELISA specific for hMANF.[76] Briefly, a 96-well MaxiSorp plate (Thermo Fisher) was coated with an anti-hMANF antibody. Samples from developing cortical neurons were incubated overnight at +4°C. Horseradish-peroxidase-linked anti-hMANF antibody was used for detection. Color was developed using the DuoSet ELISA Development System (R&D). The hMANF concentration was normalized to protein concentration determined by the Lowry method (DC Protein Assay, Bio-Rad).

SVZ Explant Cultures

Cultures were prepared from postnatal day (P) 3–5 mice. Brains were dissected and ≈ 0.1 mm^3 pieces of the SVZ were cultured on Matrigel (Corning) coated 96-well plates (Neurobasal medium; 2% B27 supplement; 2 mM GlutaMAX; and penicillin-streptomycin 50 U/mL, Gibco). Cultured explants were treated with BDNF or MANF from days 1 to 4. Cell migration distance was examined on days 1, 4, and 7. Explants were transduced with LV-hDCX-GFP, LV-hDCX-myrAkt-GFP, or LV-hDCX-hMANF-IRES-GFP on day 1 and cell migration distance was examined on day 1 and 6. At the end of the experiment, explants were fixed in 4% PFA. Explants were blocked with 3% donkey serum (0.2% Triton X-100 in PBS) and then incubated with primary goat anti-DCX (1:400, Santa Cruz) and rabbit anti-GFP (1:1,000, Chemicon International) antibodies for 24 hr and with secondary antibodies as described below.

Western Blotting

Explant samples were homogenized in lysis buffer (5 mM HEPES, pH 7.4; 320 mM sucrose; 1 mM EDTA; 0.1% SDS; and protease inhibitors [Roche]). Protein concentrations were determined using a BSA kit (Pierce). Samples were diluted in lysis buffer and Laemmli buffer containing 2% mercaptoethanol, and 20 μg protein was loaded on a 10% SDS-polyacrylamide gel. The nitrocellulose membrane was blocked in 5% skimmed milk and incubated with rabbit anti-β-tubulin III (Tuj1, 1:1,000, Covance), mouse anti-GFAP (1:1,000, Millipore), rabbit anti-pERK (1:1,000, Cell Signaling Technology), rabbit anti-ERK (1:1,000, Cell Signaling Technology), rabbit anti-pAkt (1:1,000, Cell Signaling Technology), rabbit anti-Akt (1:1,000, Cell Signaling Technology), rabbit anti-phospho-S6 Ribosomal protein (1:1,000, Cell Signaling Technology), rabbit anti-pSTAT3-Ser727 (1:500, Cell Signaling Technology), rabbit anti-pSTAT3-Tyr705 (1:500, Cell Signaling Technology), rabbit anti-STAT3 (1:500, Santa Cruz Biotechnology), goat anti-GRP78 (1:500, Santa Cruz Biotechnology), and mouse anti-glyceraldehyde-3-phosphate dehydrogenase (GAPDH; 1:2,000, Millipore) antibodies at 4°C overnight, and then probed with goat anti-mouse or goat anti-rabbit IR-Dye 670 or 800 secondary antibodies (LI-COR Biosciences) in 5% milk in PBS with Tween 20 (PBS-T) for 2 hr. Membranes were imaged using a LI-COR Odyssey scanner and analyzed using Odyssey 3.0 analytical software (LI-COR Biosciences, Lincoln, NE).

Animal Experiments

All animals were housed under a 12-hr "light-dark" or then "lights on and dark" cycle with ad libitum access to food and water. All experimental procedures were performed according to the 3R principles of the EU directive 2010/63/EU and local laws and regulations (Finnish Act on the Protection of Animals Used for Scientific or Educational Purposes [497/2013] and Government Decree on the Protection of Animals Used for Scientific or Educational Purposes [564/2013]). All experiments were approved by the National Animal Experiment Board (ESAVI/5459/04.10.03/2011 and ESAVI/7812/04.10.07/2015).

dMCAo

Ligation of the right middle cerebral artery (MCA) and bilateral common carotid arteries (CCAs) was performed on adult male Sprague-Dawley rats (220–260 g, Envigo) under chloral hydrate (0.4 g/kg intraperitoneally [i.p.]) anesthesia as described.[77,78] Briefly, bilateral CCAs were isolated through a ventral midline cervical incision. Rats were placed in a stereotaxic apparatus and a craniotomy was made over the right hemisphere. The right MCA was ligated with a 10-0 suture, and bilateral CCAs were ligated with arterial clamps for 90 min. After 90 min of ischemia, the suture around the MCA and arterial clips was removed. After recovery from anesthesia, the rats were returned to their home cage. Core temperature was maintained at 37°C. In experiments comparing the effect of GDNF and MANF on SVZ cells, the animals were examined using the Bederson's neurological test and body-asymmetry analysis 2 days after dMCAo. Behavioral analysis was carried out in a blinded fashion, and the experimenter did not know any surgical information. On the basis of the scores, the animals were then divided into three groups, keeping the average score of the three groups equal. On day 3, 7, and 10 after dMCAo surgery, hGDNF protein (10 μg), rhMANF protein (10 μg), or PBS was injected into the right lateral ventricle with the stereotaxic coordinates A/P −0.3; L/M +1.3; D/V −4.5 (from the surface of the skull) under isoflurane anesthesia. 4 μL solution was injected at a rate of 0.5 μL/min, and the needle (WPI nanofil 33G) was retained in place for 5 min after the injection.

To explore the long-term effect of MANF on the infarct boundary, 20 rats were implanted with infusion cannulas connected to subcutaneously placed osmotic minipumps (Alzet model 2002, Durect, CA,

USA) into the peri-infarction zone, with coordinates A/P −0.5; L/M +1.9; D/V −2.5, and secured to the skull using three stainless steel screws and polycarboxylate cement (Aqualox; VOCO, Germany). Pumps were filled with recombinant human GDNF, MANF (0.25 μg/μL), or PBS from post-stroke day 3 to day 16 (12 μL/day), after which the pumps were removed.

BrdU Injections

To study the effect of GDNF and MANF on proliferation of NSCs and NPCs, BrdU (50 mg/kg) was administered i.p. twice per day on days 3–10 after dMCAo (Figure 7A). In order to study the migration and differentiation of NPCs, i.p. injections of BrdU (50 mg/kg) were administered 3 times, with 2 hr intervals at day 2 after dMCAo before long-term GDNF or MANF infusion.

Immunofluorescence Staining

Cells or SVZ explant cultures cells were permeabilized for 15 min with 0.1% Triton X-100 in PBS and blocked for 1 hr with PBS containing 0.1% Triton X-100, 2% BSA, and 5% horse serum. Cells or explants were then incubated overnight with rabbit anti-MANF (1:1,000, Icosagen), rabbit anti-GFP (1:1,000, Life Technologies), or goat anti-DCX (1:400, DCX; Santa Cruz Biotechnology) in PBS containing 0.1% Triton X-100 and 5% normal horse serum at 4°C with gentle shaking, followed by 1 hr incubation with corresponding Alexa Fluor 488- or 568-conjugated secondary antibodies (1:500, Life Technologies). Finally, cells were stained with 5 μg/mL solution of DAPI (Sigma-Aldrich) in PBS. Fluorescence images were captured with Cellomics CellInsight (Thermo Scientific) equipped with Olympus UPlanFL N 10×/0.3 and Olympus LUCPlanFL N 20×/0.45 objectives and acquired with the CellProfiler project 2.1.1 software.[79,80] For SVZ explant cultures, the migration distance of migratory chains was measured for DCX^+ cells using ImageJ software. The three longest migratory chains per explant were used to estimate the maximum migration distance.

Histology, Immunohistochemical, and Immunofluorescent Staining of Brain Sections

Brains were fixed in 4% PFA and embedded in paraffin. Brains were sectioned into 5-μm-thick coronal or sagittal sections. Slides were deparaffinized and re-hydrated through a graded alcohol series before being subjected to antigen retrieval in 10 mM sodium citrate buffer, pH 6.0, or 0.05% citraconic anhydride buffer, pH 7.4, at 120°C for 10 min. The sections were incubated with one of the following primary antibodies: rabbit anti-MANF (Isocagen, 1:1,000), goat anti-DCX (Santa Cruz, 1:400), mouse anti-Nestin (Millipore, 1:400), sheep anti-BrdU (Abcam, 1:200), mouse anti-GFAP (Millipore, 1:500), mouse anti-NeuN (Millipore,1:400), rabbit anti-GFAP (Sigma-Aldrich, 1:500), and mouse anti-NG2 (Millipore, 1:200) in TBS-T with 5% serum chosen based on the secondary antibody at 4°C overnight. For immunofluorescent staining, appropriate secondary antibodies conjugated to Alexa Fluor 488 or 568 (Life Technologies, 1:500) were used. Fluorescence images were captured with a Zeiss AxioImager M2 482 epifluorescence microscope equipped with a 483 AxioCam HRm camera. Images were acquired with the AxioVision4 software. For immunohistochemistry, biotinylated secondary antibody and peroxidase-conjugated streptavidin Vectastain ABC-detection system (Vector Laboratories) were used. Sections were developed with diaminobenzidine peroxidase substrate (Vector Laboratories) and imaged with a Pannoramic 250 Flash II slide scanner (3DHistech, http://www.biocenter.helsinki.fi/bi/histoscanner/index.html).

For quantification of DCX^+ cells, three to six sections through the lesion (1.6–3.0 mm lateral to the bregma) were examined. The interval between the sections was 0.5 mm. For quantification of BrdU immunofluorescent staining, three sections, 600 μm apart, starting at 1.6 mm lateral to the bregma, were sampled for each brain, and the number of $BrdU^+$ cells in the SVZ was counted with Image-Pro Analyzer 7.0. Double immunofluorescence (BrdU/DCX, BrdU/GFAP, and BrdU/NG2) was quantified from images taken at 20 × magnification. For quantification of neuronal differentiation ($BrdU^+/NeuN^+$ cells), immunofluorescence images were taken from five sections beginning at 2.0 mm anterior to the bregma and until 0.0 mm. The images were taken at 40 × magnification with a 400 μm interval.

Statistical Analysis

Values are presented as mean ± SEM. Unpaired Student's t test and ANOVA with Fisher's LSD or Tukey's post hoc test were used for statistical analysis. A statistically significant difference was defined as $p < 0.05$.

SUPPLEMENTAL INFORMATION

Supplemental Information includes one figure and one table and can be found with this article online at https://doi.org/10.1016/j.ymthe.2017.09.019.

AUTHOR CONTRIBUTIONS

K.T.: conception and design, collection and assembly of data, data analysis and interpretation, manuscript writing, and final approval of the manuscript; J.E.A.: collection or assembly of data, provision of study material, and writing and final approval of the manuscript; A.D.: manuscript writing, final approval of the manuscript, and design and planning of NSC experiments and lentivirus vectors; K.K.: design and making the LV construct and writing and final approval of the manuscript; R.K.T.: designing the experiments, manuscript writing, and final approval of the manuscript; M.L.: design and production of MANF ko mice, manuscript writing, and final approval of the manuscript; M.A.: conception and design, data analysis, manuscript writing, financial support, and writing and final approval of the manuscript.

CONFLICTS OF INTEREST

The authors declare no conflict of interests.

ACKNOWLEDGMENTS

We thank Congjun Zheng for primary cell cultures and M.Sc. Katrina Albert and Ph.D. Sandya Narayanswami for proofreading the

manuscript. We thank Mart Saarma for his constructive comments to the manuscript and support. This work was supported by Academy of Finland grants 287843 (to A.D.) and 250275, 256398, 281394, and 309489 (to M.A.), TEKES 3iRegeneration, the Sigrid Juselius Foundation, and the Instrumentarium Science Foundation.

REFERENCES

1. Aimone, J.B., Li, Y., Lee, S.W., Clemenson, G.D., Deng, W., and Gage, F.H. (2014). Regulation and function of adult neurogenesis: from genes to cognition. Physiol. Rev. *94*, 991–1026.
2. Tobin, M.K., Bonds, J.A., Minshall, R.D., Pelligrino, D.A., Testai, F.D., and Lazarov, O. (2014). Neurogenesis and inflammation after ischemic stroke: what is known and where we go from here. J. Cereb. Blood Flow Metab. *34*, 1573–1584.
3. Ming, G.L., and Song, H. (2011). Adult neurogenesis in the mammalian brain: significant answers and significant questions. Neuron *70*, 687–702.
4. Lepousez, G., Valley, M.T., and Lledo, P.M. (2013). The impact of adult neurogenesis on olfactory bulb circuits and computations. Annu. Rev. Physiol. *75*, 339–363.
5. Ihrie, R.A., and Alvarez-Buylla, A. (2011). Lake-front property: a unique germinal niche by the lateral ventricles of the adult brain. Neuron *70*, 674–686.
6. Kokaia, Z., and Lindvall, O. (2003). Neurogenesis after ischaemic brain insults. Curr. Opin. Neurobiol. *13*, 127–132.
7. Barkho, B.Z., and Zhao, X. (2011). Adult neural stem cells: response to stroke injury and potential for therapeutic applications. Curr. Stem Cell Res. Ther. *6*, 327–338.
8. Thored, P., Wood, J., Arvidsson, A., Cammenga, J., Kokaia, Z., and Lindvall, O. (2007). Long-term neuroblast migration along blood vessels in an area with transient angiogenesis and increased vascularization after stroke. Stroke *38*, 3032–3039.
9. Parent, J.M., Vexler, Z.S., Gong, C., Derugin, N., and Ferriero, D.M. (2002). Rat forebrain neurogenesis and striatal neuron replacement after focal stroke. Ann. Neurol. *52*, 802–813.
10. Kreuzberg, M., Kanov, E., Timofeev, O., Schwaninger, M., Monyer, H., and Khodosevich, K. (2010). Increased subventricular zone-derived cortical neurogenesis after ischemic lesion. Exp. Neurol. *226*, 90–99.
11. Arvidsson, A., Collin, T., Kirik, D., Kokaia, Z., and Lindvall, O. (2002). Neuronal replacement from endogenous precursors in the adult brain after stroke. Nat. Med. *8*, 963–970.
12. Luo, Y., Kuo, C.C., Shen, H., Chou, J., Greig, N.H., Hoffer, B.J., and Wang, Y. (2009). Delayed treatment with a p53 inhibitor enhances recovery in stroke brain. Ann. Neurol. *65*, 520–530.
13. Airaksinen, M.S., and Saarma, M. (2002). The GDNF family: signalling, biological functions and therapeutic value. Nat. Rev. Neurosci. *3*, 383–394.
14. Gordon, T. (2009). The role of neurotrophic factors in nerve regeneration. Neurosurg. Focus *26*, E3.
15. Pozas, E., and Ibáñez, C.F. (2005). GDNF and GFRalpha1 promote differentiation and tangential migration of cortical GABAergic neurons. Neuron *45*, 701–713.
16. Paratcha, G., Ibáñez, C.F., and Ledda, F. (2006). GDNF is a chemoattractant factor for neuronal precursor cells in the rostral migratory stream. Mol. Cell. Neurosci. *31*, 505–514.
17. Marks, C., Belluscio, L., and Ibáñez, C.F. (2012). Critical role of GFRα1 in the development and function of the main olfactory system. J. Neurosci. *32*, 17306–17320.
18. Kobayashi, T., Ahlenius, H., Thored, P., Kobayashi, R., Kokaia, Z., and Lindvall, O. (2006). Intracerebral infusion of glial cell line-derived neurotrophic factor promotes striatal neurogenesis after stroke in adult rats. Stroke *37*, 2361–2367.
19. Schäbitz, W.R., Steigleder, T., Cooper-Kuhn, C.M., Schwab, S., Sommer, C., Schneider, A., and Kuhn, H.G. (2007). Intravenous brain-derived neurotrophic factor enhances poststroke sensorimotor recovery and stimulates neurogenesis. Stroke *38*, 2165–2172.
20. Yu, S.J., Tseng, K.Y., Shen, H., Harvey, B.K., Airavaara, M., and Wang, Y. (2013). Local administration of AAV-BDNF to subventricular zone induces functional recovery in stroke rats. PLoS One *8*, e81750.
21. Mizobuchi, N., Hoseki, J., Kubota, H., Toyokuni, S., Nozaki, J., Naitoh, M., Koizumi, A., and Nagata, K. (2007). ARMET is a soluble ER protein induced by the unfolded protein response via ERSE-II element. Cell Struct. Funct. *32*, 41–50.
22. Apostolou, A., Shen, Y., Liang, Y., Luo, J., and Fang, S. (2008). Armet, a UPR-upregulated protein, inhibits cell proliferation and ER stress-induced cell death. Exp. Cell Res. *314*, 2454–2467.
23. Glembotski, C.C., Thuerauf, D.J., Huang, C., Vekich, J.A., Gottlieb, R.A., and Doroudgar, S. (2012). Mesencephalic astrocyte-derived neurotrophic factor protects the heart from ischemic damage and is selectively secreted upon sarco/endoplasmic reticulum calcium depletion. J. Biol. Chem. *287*, 25893–25904.
24. Henderson, M.J., Richie, C.T., Airavaara, M., Wang, Y., and Harvey, B.K. (2013). Mesencephalic astrocyte-derived neurotrophic factor (MANF) secretion and cell surface binding are modulated by KDEL receptors. J. Biol. Chem. *288*, 4209–4225.
25. Lindholm, P., Voutilainen, M.H., Laurén, J., Peränen, J., Leppänen, V.M., Andressoo, J.O., Lindahl, M., Janhunen, S., Kalkkinen, N., Timmusk, T., et al. (2007). Novel neurotrophic factor CDNF protects and rescues midbrain dopamine neurons in vivo. Nature *448*, 73–77.
26. Lindholm, P., Peränen, J., Andressoo, J.O., Kalkkinen, N., Kokaia, Z., Lindvall, O., Timmusk, T., and Saarma, M. (2008). MANF is widely expressed in mammalian tissues and differently regulated after ischemic and epileptic insults in rodent brain. Mol. Cell. Neurosci. *39*, 356–371.
27. Lindahl, M., Danilova, T., Palm, E., Lindholm, P., Võikar, V., Hakonen, E., Ustinov, J., Andressoo, J.O., Harvey, B.K., Otonkoski, T., et al. (2014). MANF is indispensable for the proliferation and survival of pancreatic β cells. Cell Rep. *7*, 366–375.
28. Airavaara, M., Shen, H., Kuo, C.C., Peränen, J., Saarma, M., Hoffer, B., and Wang, Y. (2009). Mesencephalic astrocyte-derived neurotrophic factor reduces ischemic brain injury and promotes behavioral recovery in rats. J. Comp. Neurol. *515*, 116–124.
29. Airavaara, M., Chiocco, M.J., Howard, D.B., Zuchowski, K.L., Peränen, J., Liu, C., Fang, S., Hoffer, B.J., Wang, Y., and Harvey, B.K. (2010). Widespread cortical expression of MANF by AAV serotype 7: localization and protection against ischemic brain injury. Exp. Neurol. *225*, 104–113.
30. Neves, J., Zhu, J., Sousa-Victor, P., Konjikusic, M., Riley, R., Chew, S., Qi, Y., Jasper, H., and Lamba, D.A. (2016). Immune modulation by MANF promotes tissue repair and regenerative success in the retina. Science *353*, aaf3646.
31. Voutilainen, M.H., De Lorenzo, F., Stepanova, P., Back, S., Yu, L.Y., Lindholm, P., Pörsti, E., Saarma, M., Männistö, P.T., and Tuominen, R.K. (2017). Evidence for an additive neurorestorative effect of simultaneously administered CDNF and GDNF in hemiparkinsonian rats: implications for different mechanism of action. eNeuro *4*.
32. Hao, F., Yang, C., Chen, S.S., Wang, Y.Y., Zhou, W., Hao, Q., Lu, T., Hoffer, B., Zhao, L.R., Duan, W.M., et al. (2017). Long-term protective effects of AAV9-mesencephalic astrocyte-derived neurotrophic factor gene transfer in parkinsonian rats. Exp. Neurol. *291*, 120–133.
33. Hellman, M., Arumäe, U., Yu, L.Y., Lindholm, P., Peränen, J., Saarma, M., and Permi, P. (2011). Mesencephalic astrocyte-derived neurotrophic factor (MANF) has a unique mechanism to rescue apoptotic neurons. J. Biol. Chem. *286*, 2675–2680.
34. Voutilainen, M.H., Bäck, S., Pörsti, E., Toppinen, L., Lindgren, L., Lindholm, P., Peränen, J., Saarma, M., and Tuominen, R.K. (2009). Mesencephalic astrocyte-derived neurotrophic factor is neurorestorative in rat model of Parkinson's disease. J. Neurosci. *29*, 9651–9659.
35. Ries, V., Henchcliffe, C., Kareva, T., Rzhetskaya, M., Bland, R., During, M.J., Kholodilov, N., and Burke, R.E. (2006). Oncoprotein Akt/PKB induces trophic effects in murine models of Parkinson's disease. Proc. Natl. Acad. Sci. USA *103*, 18757–18762.
36. Dempsey, R.J., Sailor, K.A., Bowen, K.K., Türeyen, K., and Vemuganti, R. (2003). Stroke-induced progenitor cell proliferation in adult spontaneously hypertensive rat brain: effect of exogenous IGF-1 and GDNF. J. Neurochem. *87*, 586–597.

37. Mätlik, K., Yu, L.Y., Eesmaa, A., Hellman, M., Lindholm, P., Peränen, J., Galli, E., Anttila, J., Saarma, M., Permi, P., et al. (2015). Role of two sequence motifs of mesencephalic astrocyte-derived neurotrophic factor in its survival-promoting activity. Cell Death Dis. *6*, e2032.

38. Petrova, P., Raibekas, A., Pevsner, J., Vigo, N., Anafi, M., Moore, M.K., Peaire, A.E., Shridhar, V., Smith, D.I., Kelly, J., et al. (2003). MANF: a new mesencephalic, astrocyte-derived neurotrophic factor with selectivity for dopaminergic neurons. J. Mol. Neurosci. *20*, 173–188.

39. Lindahl, M., Saarma, M., and Lindholm, P. (2017). Unconventional neurotrophic factors CDNF and MANF: Structure, physiological functions and therapeutic potential. Neurobiol. Dis. *97* (Pt B), 90–102.

40. Palgi, M., Lindström, R., Peränen, J., Piepponen, T.P., Saarma, M., and Heino, T.I. (2009). Evidence that DmMANF is an invertebrate neurotrophic factor supporting dopaminergic neurons. Proc. Natl. Acad. Sci. USA *106*, 2429–2434.

41. Lindberg, O.R., Brederlau, A., Jansson, A., Nannmark, U., Cooper-Kuhn, C., and Kuhn, H.G. (2012). Characterization of epidermal growth factor-induced dysplasia in the adult rat subventricular zone. Stem Cells Dev. *21*, 1356–1366.

42. Lindberg, O.R., Brederlau, A., and Kuhn, H.G. (2014). Epidermal growth factor treatment of the adult brain subventricular zone leads to focal microglia/macrophage accumulation and angiogenesis. Stem Cell Reports *2*, 440–448.

43. Yang, S., Huang, S., Gaertig, M.A., Li, X.J., and Li, S. (2014). Age-dependent decrease in chaperone activity impairs MANF expression, leading to Purkinje cell degeneration in inducible SCA17 mice. Neuron *81*, 349–365.

44. Gartsbein, M., Alt, A., Hashimoto, K., Nakajima, K., Kuroki, T., and Tennenbaum, T. (2006). The role of protein kinase C delta activation and STAT3 Ser727 phosphorylation in insulin-induced keratinocyte proliferation. J. Cell Sci. *119*, 470–481.

45. Corbit, K.C., Soh, J.W., Yoshida, K., Eves, E.M., Weinstein, I.B., and Rosner, M.R. (2000). Different protein kinase C isoforms determine growth factor specificity in neuronal cells. Mol. Cell. Biol. *20*, 5392–5403.

46. Yu, H., Pardoll, D., and Jove, R. (2009). STATs in cancer inflammation and immunity: a leading role for STAT3. Nat. Rev. Cancer *9*, 798–809.

47. Bauer, S. (2009). Cytokine control of adult neural stem cells. Ann. N Y Acad. Sci. *1153*, 48–56.

48. Islam, O., Gong, X., Rose-John, S., and Heese, K. (2009). Interleukin-6 and neural stem cells: more than gliogenesis. Mol. Biol. Cell *20*, 188–199.

49. Xia, X.G., Hofmann, H.D., Deller, T., and Kirsch, M. (2002). Induction of STAT3 signaling in activated astrocytes and sprouting septal neurons following entorhinal cortex lesion in adult rats. Mol. Cell. Neurosci. *21*, 379–392.

50. Herrmann, J.E., Imura, T., Song, B., Qi, J., Ao, Y., Nguyen, T.K., Korsak, R.A., Takeda, K., Akira, S., and Sofroniew, M.V. (2008). STAT3 is a critical regulator of astrogliosis and scar formation after spinal cord injury. J. Neurosci. *28*, 7231–7243.

51. Kang, M.J., Park, S.Y., and Han, J.S. (2016). Hippocalcin is required for astrocytic differentiation through activation of Stat3 in hippocampal neural precursor cells. Front. Mol. Neurosci. *9*, 110.

52. Ng, D.C., Lin, B.H., Lim, C.P., Huang, G., Zhang, T., Poli, V., and Cao, X. (2006). Stat3 regulates microtubules by antagonizing the depolymerization activity of stathmin. J. Cell Biol. *172*, 245–257.

53. Zhou, L., and Too, H.P. (2011). Mitochondrial localized STAT3 is involved in NGF induced neurite outgrowth. PLoS One *6*, e21680.

54. Sheu, J.Y., Kulhanek, D.J., and Eckenstein, F.P. (2000). Differential patterns of ERK and STAT3 phosphorylation after sciatic nerve transection in the rat. Exp. Neurol. *166*, 392–402.

55. Huang, C., Jacobson, K., and Schaller, M.D. (2004). MAP kinases and cell migration. J. Cell Sci. *117*, 4619–4628.

56. Anand-Apte, B., Zetter, B.R., Viswanathan, A., Qiu, R.G., Chen, J., Ruggieri, R., and Symons, M. (1997). Platelet-derived growth factor and fibronectin-stimulated migration are differentially regulated by the Rac and extracellular signal-regulated kinase pathways. J. Biol. Chem. *272*, 30688–30692.

57. Webb, D.J., Donais, K., Whitmore, L.A., Thomas, S.M., Turner, C.E., Parsons, J.T., and Horwitz, A.F. (2004). FAK-Src signalling through paxillin, ERK and MLCK regulates adhesion disassembly. Nat. Cell Biol. *6*, 154–161.

58. Chen, P., Murphy-Ullrich, J.E., and Wells, A. (1996). A role for gelsolin in actuating epidermal growth factor receptor-mediated cell motility. J. Cell Biol. *134*, 689–698.

59. Giroux, S., Tremblay, M., Bernard, D., Cardin-Girard, J.F., Aubry, S., Larouche, L., Rousseau, S., Huot, J., Landry, J., Jeannotte, L., et al. (1999). Embryonic death of Mek1-deficient mice reveals a role for this kinase in angiogenesis in the labyrinthine region of the placenta. Curr. Biol. *9*, 369–372.

60. Sakata, H., Narasimhan, P., Niizuma, K., Maier, C.M., Wakai, T., and Chan, P.H. (2012). Interleukin 6-preconditioned neural stem cells reduce ischaemic injury in stroke mice. Brain *135*, 3298–3310.

61. Zhao, H., Cheng, L., Du, X., Hou, Y., Liu, Y., Cui, Z., and Nie, L. (2016). Transplantation of cerebral dopamine neurotrophic factor transducted BMSCs in contusion spinal cord injury of rats: promotion of nerve regeneration by alleviating neuroinflammation. Mol. Neurobiol. *53*, 187–199.

62. Chapman, K.Z., Ge, R., Monni, E., Tatarishvili, J., Ahlenius, H., Arvidsson, A., Ekdahl, C.T., Lindvall, O., and Kokaia, Z. (2015). Inflammation without neuronal death triggers striatal neurogenesis comparable to stroke. Neurobiol. Dis. *83*, 1–15.

63. Alam, M.A., Subramanyam Rallabandi, V.P., and Roy, P.K. (2016). Systems biology of immunomodulation for post-stroke neuroplasticity: multimodal implications of pharmacotherapy and neurorehabilitation. Front. Neurol. *7*, 94.

64. Chen, L., Feng, L., Wang, X., Du, J., Chen, Y., Yang, W., Zhou, C., Cheng, L., Shen, Y., Fang, S., et al. (2015). Mesencephalic astrocyte-derived neurotrophic factor is involved in inflammation by negatively regulating the NF-κB pathway. Sci. Rep. *5*, 8133.

65. Stratoulias, V., and Heino, T.I. (2015). MANF silencing, immunity induction or autophagy trigger an unusual cell type in metamorphosing Drosophila brain. Cell. Mol. Life Sci. *72*, 1989–2004.

66. Shen, Y., Sun, A., Wang, Y., Cha, D., Wang, H., Wang, F., Feng, L., Fang, S., and Shen, Y. (2012). Upregulation of mesencephalic astrocyte-derived neurotrophic factor in glial cells is associated with ischemia-induced glial activation. J. Neuroinflammation *9*, 254.

67. Lahti, L., Saarimäki-Vire, J., Rita, H., and Partanen, J. (2011). FGF signaling gradient maintains symmetrical proliferative divisions of midbrain neuronal progenitors. Dev. Biol. *349*, 270–282.

68. Saarimäki-Vire, J., Peltopuro, P., Lahti, L., Naserke, T., Blak, A.A., Vogt Weisenhorn, D.M., Yu, K., Ornitz, D.M., Wurst, W., and Partanen, J. (2007). Fibroblast growth factor receptors cooperate to regulate neural progenitor properties in the developing midbrain and hindbrain. J. Neurosci. *27*, 8581–8592.

69. Kalluri, H.S., Eickstaedt, J., and Dempsey, R.J. (2007). Oxygen glucose deprivation inhibits the growth and ERK phosphorylation of neural progenitor cells in vitro. Neurosci. Lett. *426*, 145–148.

70. Riccardi, C., and Nicoletti, I. (2006). Analysis of apoptosis by propidium iodide staining and flow cytometry. Nat. Protoc. *1*, 1458–1461.

71. Liu, X., Constantinescu, S.N., Sun, Y., Bogan, J.S., Hirsch, D., Weinberg, R.A., and Lodish, H.F. (2000). Generation of mammalian cells stably expressing multiple genes at predetermined levels. Anal. Biochem. *280*, 20–28.

72. Garcia-Gonzalez, D., Khodosevich, K., Watanabe, Y., Rollenhagen, A., Lubke, J.H.R., and Monyer, H. (2017). Serotonergic projections govern postnatal neuroblast migration. Neuron *94*, 534–549.

73. Khodosevich, K., Zuccotti, A., Kreuzberg, M.M., Le Magueresse, C., Frank, M., Willecke, K., and Monyer, H. (2012). Connexin45 modulates the proliferation of transit-amplifying precursor cells in the mouse subventricular zone. Proc. Natl. Acad. Sci. USA *109*, 20107–20112.

74. Ding, B., and Kilpatrick, D.L. (2013). Lentiviral vector production, titration, and transduction of primary neurons. Methods Mol. Biol. *1018*, 119–131.

75. Li, L., and Hu, G.K. (2015). Pink1 protects cortical neurons from thapsigargin-induced oxidative stress and neuronal apoptosis. Biosci. Rep. *35*.

76. Galli, E., Härkönen, T., Sainio, M.T., Ustav, M., Toots, U., Urtti, A., Yliperttula, M., Lindahl, M., Knip, M., Saarma, M., et al. (2016). Increased circulating concentrations of mesencephalic astrocyte-derived neurotrophic factor in children with type 1 diabetes. Sci. Rep. *6*, 29058.

77. Chen, S.T., Hsu, C.Y., Hogan, E.L., Maricq, H., and Balentine, J.D. (1986). A model of focal ischemic stroke in the rat: reproducible extensive cortical infarction. Stroke *17*, 738–743.

78. Mätlik, K., Abo-Ramadan, U., Harvey, B.K., Arumäe, U., and Airavaara, M. (2014). AAV-mediated targeting of gene expression to the peri-infarct region in rat cortical stroke model. J. Neurosci. Methods *236*, 107–113.

79. Kamentsky, L., Jones, T.R., Fraser, A., Bray, M.A., Logan, D.J., Madden, K.L., Ljosa, V., Rueden, C., Eliceiri, K.W., and Carpenter, A.E. (2011). Improved structure, function and compatibility for CellProfiler: modular high-throughput image analysis software. Bioinformatics *27*, 1179–1180.

80. Jones, T.R., Carpenter, A.E., Lamprecht, M.R., Moffat, J., Silver, S.J., Grenier, J.K., Castoreno, A.B., Eggert, U.S., Root, D.E., Golland, P., et al. (2009). Scoring diverse cellular morphologies in image-based screens with iterative feedback and machine learning. Proc. Natl. Acad. Sci. USA *106*, 1826–1831.

YMTHE, Volume *26*

Supplemental Information

MANF Promotes Differentiation and Migration of Neural Progenitor Cells with Potential Neural Regenerative Effects in Stroke

Kuan-Yin Tseng, Jenni E. Anttila, Konstantin Khodosevich, Raimo K. Tuominen, Maria Lindahl, Andrii Domanskyi, and Mikko Airavaara

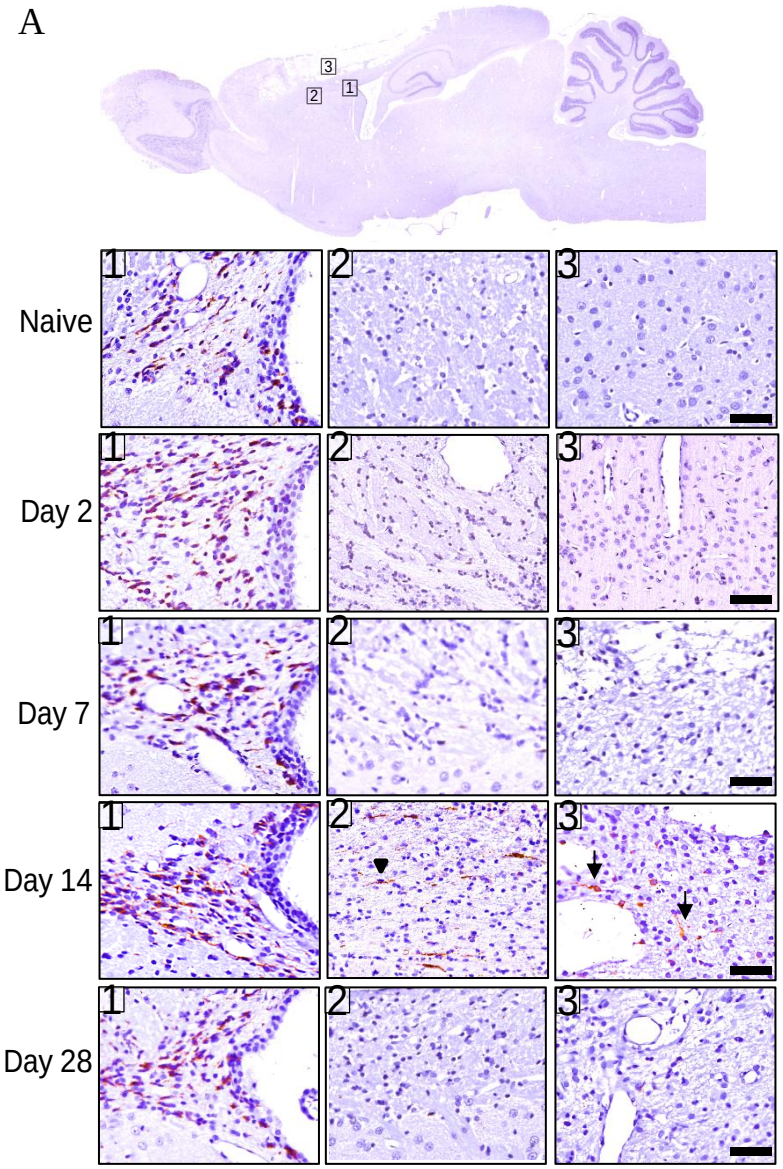

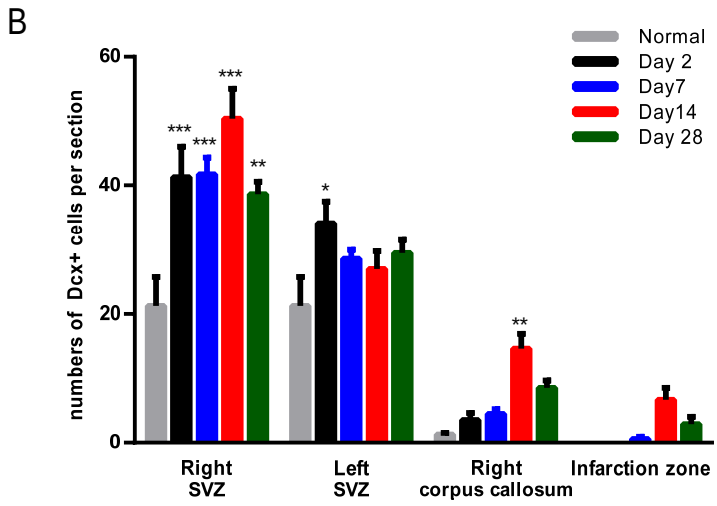

Supp. Fig.1. A, Distribution of DCX$^+$ cells in the SVZ, corpus callosum beneath the lesion area, and infarction zone at different time points after dMCAo. DCX$^+$ cells in the infarction zone and underlying white matter exhibit morphology characterized by leading and trailing processes (arrow). **B,** Quantification of the number of DCX$^+$ cells in different brain areas at different time points after stroke reveals a significant increase in the number of DCX$^+$ cells at 2 to 28 days post-stroke in the right SVZ compared to non-lesioned SVZ. A significant increase of DCX$^+$ cells was also found in the corpus callosum at post-injury day 14 rats compared to other post-stroke days (n=3-4, 2-way ANOVA time x brain area $p<0.001$; *** $p<0.001$, * $p<0.05$ Tukey's post hoc test, scale bar 50 µm.

Details of the used antibodies.

Antibody Name	Vendor	Cat Num.	Proper Citation	Clonality	Host Organism
Purified anti-Tubulin -3 (TUBB3) Antibody	BioLegend	802001	(BioLegend Cat# 802001, RRID: AB_2564645)	polyclonal antibody	rabbit
Anti-Glial Fibrillary Acidic Protein, clone GA5 antibody	Millipore	MAB360	(Millipore Cat# MAB360, RRID: AB_11212597)	monoclonal antibody	mouse
Phospho-p44/42 MAPK (Erk1/2) (Thr202/Tyr204) (20G11) Rabbit mAb antibody	Cell Signaling Technology	4376S	(Cell Signaling Technology Cat# 4376S, RRID: AB_331772)	monoclonal antibody	rabbit
Map Kinase, p44/42, Erk1/Erk2 antibody	Cell Signaling Technology	4695	(Cell Signaling Technology Cat# 4695, RRID: AB_390779)	monoclonal antibody	rabbit
Phospho-Akt (Thr308) Antibody	Cell Signaling Technology	9275 also 9275S, 9275L	(Cell Signaling Technology Cat# 9275, RRID: AB_329828)	polyclonal antibody	rabbit
Akt Antibody	Cell Signaling Technology	9272 also 9272S	(Cell Signaling Technology Cat# 9272, RRID: AB_329827)	polyclonal antibody	rabbit
Phospho-S6 Ribosomal Protein (Ser235/236) Antibody	Cell Signaling Technology	2211 also 2211L, 2211S	(Cell Signaling Technology Cat# 2211, RRID: AB_331679)	polyclonal antibody	rabbit
GRP 78 (C-20) antibody	Santa Cruz Biotechnology	sc-1051	(Santa Cruz Biotechnology Cat# sc-1051, RRID: AB_2119994)	polyclonal antibody	goat
Phospho-Stat3 (Ser727) Antibody	Cell Signaling Technology	9134 also 9134S, 9134L	(Cell Signaling Technology Cat# 9134, RRID: AB_331589)	polyclonal antibody	rabbit
Phospho-Stat-3 (tyr705) antibody	Cell Signaling Technology	9131 also 9131S, 9131L	(Cell Signaling Technology Cat# 9131, RRID: AB_331586)	polyclonal antibody	rabbit
Rabbit Anti-Stat3 Polyclonal antibody, Unconjugated	Santa Cruz Biotechnology	sc-482	(Santa Cruz Biotechnology Cat# sc-482, RRID: AB_632440)	polyclonal antibody	rabbit
Mouse Anti-Glyceraldehyde-3-PDH	Millipore	MAB374	(Millipore Cat# MAB374, RRID: AB_2107445)	monoclonal antibody	mouse

(GAPDH) Monoclonal antibody, Unconjugated					
Mouse monoclonal antibody to human MANF (Mesencephalic astrocyte-derived neurotrophic factor)	Icosagen AS	Icosagen AS	(Icosagen AS Cat# 310-100, RRID: AB_11135308)	polyclonal antibody	rabbit
Doublecortin (C-18) antibody	Santa Cruz Biotechnology	sc-8066	(Santa Cruz Biotechnology Cat# sc-8066, RRID: AB_2088494)	polyclonal antibody	goat
Mouse Anti-Nestin Monoclonal antibody, Unconjugated, Clone rat-401	Millipore	MAB353	(Millipore Cat# MAB353, RRID: AB_94911)	monoclonal antibody	mouse
Sheep Anti-BrdU Polyclonal Antibody, Unconjugated	Abcam	ab1893	(Abcam Cat# ab1893, RRID: AB_302659)	polyclonal antibody	sheep
Anti-NeuN, clone A60 antibody	Millipore	MAB377	(Millipore Cat# MAB377, RRID: AB_2298772)	monoclonal antibody	mouse
Anti-GFAP, N-Terminal antibody produced in rabbit	Sigma-Aldrich	SAB4501162	(Sigma-Aldrich Cat# SAB4501162, RRID: AB_10746077)	polyclonal antibody	rabbit
Mouse Anti-NG2 Monoclonal antibody, Unconjugated, Clone 132.38	Millipore	05-710	(Millipore Cat# 05-710, RRID: AB_309925)	monoclonal antibody	mouse
Rabbit Anti-Green Fluorescent Protein (GFP) Polyclonal Antibody, Unconjugated	Thermo Fisher Scientific	A-6455	(Thermo Fisher Scientific Cat# A-6455, RRID: AB_221570)	polyclonal antibody	rabbit